Aus der Klinik für Neurologie

der Medizinischen Fakultät Charité – Universitätsmedizin Berlin

DISSERTATION

„Effects of physical activity and nutrition on neuronal plasticity, neurogenesis and cognition in the healthy brain and in a mouse model of Parkinson's disease"

zur Erlangung des akademischen Grades

Doctor of Philosophy (PhD)

vorgelegt der Medizinischen Fakultät

Charité – Universitätsmedizin Berlin

von

Charlotte Klein

aus Mettingen

Datum der Promotion: 9. Dezember 2016

List of Abbreviations

AD	Alzheimer's disease
BDNF	Brain-derived neurotrophic factor
BrdU	5'-bromo-2'-deoxyuridine
BW	Body weight
CD	Control diet
cm	Centimeter
CTR	Control
D	Dimension
DAB	3,3'-Diaminobenzidine
DCX	Doublecortin
DG	Dentate gyrus
DIR	Direct experience of enriched environment
DNA	Deoxyribonucleic acid
ELISA	Enzyme-linked immunosorbent assay
ENR	Enriched environment
FoV	Field of view
g	gram
GFAP	Glial fibrillary acidic protein
GFP	Green fluorescent protein
h	hours
H_2O_2	Hydrogen peroxide
HCl	Hydrochloric acid
HFD	High-fat diet
Hz	Hertz
Iba1	Ionized calcium-binding adaptor molecule 1
IND	Indirect experience of enriched environment
kcal	Large calorie
kg	Kilogram
kPa	Kilopascal
L-DOPA	L-3,4-dihydroxyphenylalanine
m	Meter
mg	Milligram

mm	Millimeter
MPTP	1-methyl-4-phenyl-1,2,3,6-tetrahydropyridine
MRE	Magnetic resonance elastography
MRI	Magnetic resonance imaging
ms	millisecond
MSG	Motion sensitizing gradient
mT	Millitesla
MWM	Morris water maze
NaCl	Sodiumchloride
NeuN	Neuronal nuclei
NiCl	Nickelchloride
PBS	Phosphate-buffered saline
PD	Parkinson's disease
PFA	Paraformaldehyde
-R	-Running
s	second
-S	-Sedentary
S.E.M.	Standard error of the mean
SGZ	Subgranular zone
SN	Substantia nigra
SPECT	Single-photon emission computed tomography
T	Tesla

Abstract (English)

Parkinson's disease (PD) and obesity are associated with cognitive dysfunction. Adult hippocampal neurogenesis, the continuous generation of new neurons from resident neural precursor cells, is crucial for the maintenance of hippocampus-dependent cognitive functioning throughout life. Evidence from animal studies indicates that impaired adult neurogenesis may account for the alterations in cognitive performance, particularly spatial learning and memory, which are observed in a neurodegenerative or obese state. Lifestyle changes (physical exercise and environmental enrichment) have been shown to produce beneficial structural and functional modifications in the hippocampus. Neuropathological changes such as a dysfunctional neurogenesis often precede clinical symptoms in neurodegenerative diseases. So far, no diagnostic tool exists, which allows the early diagnosis for potentially more effective therapeutic strategies. Magnetic resonance elastography (MRE) may represent such a tool as it detects alterations in viscoelastic properties of brain tissue in patients with neurodegenerative diseases. First steps have been taken using animal models to correlate these alterations with the histopathology to identify potential markers that determine the biomechanical properties of brain tissue. Here, we evaluated the biomechanical response of the brain to altered adult hippocampal neurogenesis in the 1-methyl-4-phenyl-1,2,3,6-tetrahydropyridine (MPTP) mouse model of PD (study 1), the effects of indirect exposure to a stimulating enriched environment in healthy adult mice (study 2), which represents the passive stimulation of humans watching television, and of physical exercise in a diet-induced obesity mouse model (study 3) on hippocampal neurogenesis and hippocampus-dependent cognitive functions. Neurogenesis and brain viscoelasticity were increased at the same time point after MPTP treatment. Direct but not indirect exposure to environmental enrichment enhanced hippocampal neurogenesis and improved spatial learning and memory performance in the water maze. A high-fat diet (HFD) initiated during adolescence specifically impaired flexible memory expression in adulthood and reduced the number of immature but not mature neurons, which could be prevented by concurrent exercise. In summary, the results indicate that newly generated neurons are involved in the viscoelastic matrix of the hippocampus. This contributes to the validation of MRE biomarkers for the clinical diagnosis of neuropathological diseases associated with cognitive dysfunction. In light of the common sedentary lifestyle (excessive television watching, physical inactivity, and energy-rich diets) related to reduced cognitive functioning, the results show that direct experience of environmental enrichment is critical for producing beneficial effects on hippocampal neurogenesis and hippocampus-dependent cognitive functions, and that physical exercise represents a potential therapeutic strategy to prevent cognitive impairment associated with obesity during adolescence.

Abstract (German)

Das idiopathische Parkinsonsyndrom (IPS) und Adipositas werden mit kognitiver Fehlfunktion in Verbindung gebracht. Die adulte hippokampale Neurogenese, eine kontinuierliche Bildung neuer Neurone aus vorhandenen neuralen Vorläuferzellen, gilt als bedeutend für die lebenslange Erhaltung der hippokampusabhängigen kognitiven Funktionsfähigkeit. Erkenntnisse aus Tierstudien legen nahe, dass eine beeinträchtigte Neurogenese verantwortlich sein könnte für die veränderten kognitiven Leistungen in neurodegenerativem oder adipösem Zustand. Änderungen des Lebensstils bewirken vorteilhafte strukturelle und funktionelle Anpassungen im Hippokampus. Klinischen Symptomen gehen oft neuropathologische Veränderungen wie eine dysfunktionale Neurogenese voraus. Bis heute gibt es kein Verfahren, das eine frühzeitige Diagnose erlaubt, um effektiver zu therapieren. Die Magnetresonanzelastographie (MRE) könnte ein solches Verfahren darstellen, da sie Veränderungen der viskoelastischen Eigenschaften von Gehirngewebe bei Patienten mit neurodegenerativen Erkrankungen erkennt. Erste Schritte hinsichtlich einer Korrelation mit der Histopathologie wurden mithilfe von Tiermodellen unternommen, um potenzielle Marker für die biomechanischen Eigenschaften von Gehirngewebe identifizieren. In der vorliegenden Arbeit wurde die biomechanische Antwort des Gehirns auf veränderte adulte hippokampale Neurogenese im 1-Methyl-4-Phenyl-1,2,3,6-Tetrahydropyridin- (MPTP-) Mausmodell für Parkinson gemessen (Studie 1), sowie die Effekte der indirekten Stimulation durch eine angereicherte Umgebung (Studie 2), ähnlich dem Fernsehen beim Menschen, und von Sport in einem diätinduzierten Adipositas-Mausmodell (Studie 3) auf die Neurogenese und hippokampusabhängige kognitive Funktionen untersucht. Die Neurogenese und Gehirnviskoelastizität waren zu demselben Zeitpunkt nach MPTP erhöht. Die direkte aber nicht indirekte Erfahrung einer reizreichen Umgebung verstärkte die Neurogenese im Hippokampus und verbesserte die räumlichen Lern- und Gedächtnisfähigkeiten im Wasserlabyrinth. Eine fettreiche Ernährung ab dem heranwachsenden Alter beeinträchtigte die flexible Gedächtnisanwendung und reduzierte die Anzahl der unreifen Neurone, was durch gleichzeitigen Sport verhindert wurde. Zusammenfassend weisen die Ergebnisse darauf hin, dass neugebildete Neurone in die viskoelastische Matrix des Gehirns eingebunden werden, was zur Validierung von MRE-Biomarkern für die klinische Diagnose neurodegenerativer Erkrankungen beiträgt. Mit Blick auf den bewegungsarmen Lebensstil, der mit einer reduzierten kognitiven Funktionsfähigkeit assoziiert wird, zeigen die Ergebnisse, dass die direkte Erfahrung einer angereicherten Umgebung notwendig ist, um sich günstig auf die hippokampale Neurogenese und hippokampusabhängigen kognitiven Funktionen auszuwirken, und dass Sport eine mögliche therapeutische Strategie darstellt zur Verhinderung von kognitiven Beeinträchtigungen, die mit Adipositas im heranwachsenden Alter in Verbindung gebracht werden.

1. Introduction

Western civilization is at present characterized by a higher life expectancy but also by a lifestyle, which includes the overconsumption of energy-dense food and reduced requirements for physical activity compared to that of our hunter and gatherer ancestors. This leads to an aging society with an increased risk of obesity and resulting neuronal loss or other neurodegenerative diseases, such as Parkinson's disease (PD). Obesity is not only associated with comorbidities including type II diabetes and cardiovascular diseases (1), but also with cognitive dysfunction (2), which is likewise a dominating occurrence accompanying the characteristic motor symptoms in PD patients (3). The underlying cellular substrate of impaired cognitive functions in either pathological condition has not been yet identified but a dysfunctional adult neurogenesis in the hippocampus is one potential candidate, which has been frequently discussed (4, 5). Adult hippocampal neurogenesis is implicated in hippocampus-dependent cognitive functions (6). It describes an endogenous process during which neural precursor cells continuously proliferate and mature via several differentiation stages into neurons that are functionally integrated into existing neuronal circuits (7). This neuronal cell generation occurs at substantial levels in the subgranular zone (SGZ) of the dentate gyrus (DG) in the hippocampus and in the subventricular zone of the lateral ventricles (8). Hippocampal neurogenesis is a robustly regulated process, which can be significantly influenced by internal and external stimuli (9). An intact homeostasis of neurotransmitters, such as dopamine, has been demonstrated as one key regulator of adult neurogenesis in PD patients and in animal models (4, 10). Physical activity and environmental enrichment have been shown to be beneficial for structural and functional changes in the hippocampus. The observed increase in the number of newborn neurons in the hippocampus has been linked to the improvement of hippocampal-dependent functions, such as spatial learning and memory (11, 12). Energy-rich nutrition in turn has been shown to suppress adult hippocampal neurogenesis and to impair memory functions (13).

In neurodegenerative diseases, neuropathological changes such as a dysfunctional neurogenesis often occur long before clinical symptoms emerge (14). Therefore, a diagnosis at a preclinical stage might allow a more effective therapeutic strategy early on. In addition to the common L-DOPA test for the diagnosis of PD, [^{123}I]β-CIT and single-photon emission computed tomography ([^{123}I]β-CIT–SPECT) measure the density of the dopamine transporter in nigrostriatal neurons to evaluate the severity of the disease. These are currently the only available supportive methods for diagnosis and documentation of disease progression (15). In Alzheimer's disease (AD), both psychological tests and the visualization of pathological changes, which are generated from computed brain tomography, help to diagnose the disease but do not provide direct evidence (16). Magnetic resonance elastography (MRE) provides high specificity and resolution power and detects

alterations in viscoelastic properties of brain tissue in patients with neurodegenerative diseases (17, 18). These alterations have been shown in animal studies to correlate with cellular changes (19, 20). To this date, knowledge is very sparse of how biomechanical constants of brain tissue are related to neuronal networks in terms of cell density, cross-linking, cell differentiation and maturation states and how they are influenced in preclinical stages of neurodegenerative diseases. To expand the utility of MRE as a tool for monitoring cellular changes in the pathology of neurodegenerative diseases, we examined the biomechanical response of the brain on adult hippocampal neurogenesis as a robust correlate of neuronal plasticity in the 1-methyl-4-phenyl-1,2,3,6-tetrahydropyridine (MPTP) mouse model of PD (study 1). A sedentary lifestyle is characterized by physical inactivity and related to obesity. It is also associated with hippocampus-dependent cognitive deficits. We therefore investigated if indirect exposure and passive confrontation with a stimulating enriched environment, which mimics the human situation of television watching, would be sufficient to produce beneficial effects on hippocampal neurogenesis and hippocampus-dependent cognitive functions (study 2). We also investigated whether physical exercise can prevent or reverse cognitive impairments following an energy-dense diet and if neurogenesis is involved in this process (study 3).

2. Methodology

2.1 Animals

Female six-to-ten-weeks-old wildtype (Charles River Laboratories International, Germany; German Institute of Human Nutrition, Potsdam-Rehbrücke, Germany) and transgenic C57Bl/6N mice (Forschungseinrichtung für experimentelle Medizin, FEM, Berlin, Germany) expressing the green-fluorescent protein under the nestin promoter (Nestin-GFP) were used. The intermediate filament Nestin is exclusively produced in neural precursor cells and its coexpression with GFP helps to identify these cells (21). All mice were kept in a temperature- and humidity-controlled colony room and maintained on a light/dark cycle of 12/12 h with ad libitum access to food and water. All experiments were carried out with the permission of the responsible local authorities (*Landesamt für Gesundheit und Soziales, Berlin*) and in accordance with the European Communities Council Directive of 22nd September 2010 (2010/63/EEC). The mice were randomly assigned to the experimental groups. The investigators were blinded towards the groups.

2.2 In vivo designs

2.2.1 Study 1

A group of untreated Nestin-GFP C57Bl/6N mice (n=5) was initially measured using MRE to obtain reference (baseline) data of brain viscoelasticity. Then, MRE was applied at five time points after 0.9% Sodiumchloride (NaCl) injections (control, CTR) at 3, 6, 10, 14 and 18 days post-injection (dpi). The CTR measurements (18 dpi served as baseline for MPTP-treated mice) were followed by treatment with MPTP as described below and MRE again at equal dpi. Additional groups of untreated, NaCl- and MPTP-treated Nestin-GFP mice served as histological counterparts for baseline and the measured time points after treatment. At these timepoints, the animals (each n=5) were transcardially perfused with phosphate-buffered saline (PBS) followed by 4% paraformaldehyde (PFA) after deep anesthesia with Ketamin/Xylacine. Mice destined for histological analysis of brain tissue to quantify neurogenesis levels in the hippocampus received three injections of the mitotic marker 5'-bromo-2'-deoxyuridine (BrdU) every 24 h to label proliferating cells. Injections started on the final day of NaCl/MPTP treatment. A schematic (figure 1a) of the experimental procedure can be found in (22).

2.2.2 Study 2

Wildtype and Nestin-GFP C57Bl/6N mice were divided into two main groups. The first experienced directly an enriched environment (DIR). The second group experienced the stimulus-rich surroundings only indirectly by living in a standard cage placed in the centre of a large environmentally enriched cage (IND). Mice living in a similarly enriched cage containing an uninhabited inner cage (ENR) and mice kept in a standard cage outside of the enriched cage (CTR) served as controls. After enriched environment intervention, mice underwent behavioral testing using the Morris water maze (MWM; 23) to assess hippocampus-dependent spatial learning and memory functions. Levels of cell proliferation and the survival of newly generated cells in the hippocampus were determined. Therefore, BrdU was injected after 28 days of enriched environment either 24 h (cell proliferation in Nestin-GFP mice) or four weeks (cell survival in wildtype mice) prior to transcardial perfusion after deep anesthesia with Ketamine/Xylacine. The housing design (figure 1a) and a schematic of the experimental procedure (figure 1b) are shown in (24).

2.2.3 Study 3

Two groups of C57Bl/6N mice aged six and ten weeks respectively, were fed either a control diet (CD) or a high-fat diet (HFD) for twelve weeks. The younger (adolescent) mice had free access to a

running wheel (-R; sedentary = -S) throughout the twelve weeks of HFD (experiment 1: preventive approach). The older (young-adult) mice exercised only for 14 days after HFD (experiment 2: therapeutic approach). The two approaches mimic young physically active humans exposed to a plethora of energy-dense food and adults becoming overweight and attempting to lose weight with physical exercise. Physical activity (distance run per 24 h) was monitored throughout the exercise intervention. In each approach, mice underwent either behavioral testing after HFD and/or physical exercise intervention or were destined for histological analysis without behavioral testing to quantify hippocampal neurogenesis levels. To quantifiy the survival of newly generated neurons, BrdU was administered during the first three days of HFD or CD, respectively. Hippocampus-dependent spatial learning and memory abilities were tested using the MWM. From mice of the behavior group, native brain tissue was taken after deep anesthesia with Ketamine/Xylacine and used to determine protein levels of brain-derived neurotrophic factor (BDNF) in the hippocampus using an enzyme-linked immunosorbent assay (ELISA) kit. In (25), figure 1b illustrates the group design and figure 1a shows a schematic of the experimental procedure.

2.3 Animal models

2.3.1 1-methyl-4-phenyl-1,2,3,6-tetrahydropyridine mouse model of Parkinson's disease

Since the 1980s, when the opioid derivative MPTP attracted attention for causing irreversible Parkinsonism in drug addicts, the MPTP mouse model of PD has been used as an experimental animal model. This model replicates the characteristic dopamine deficit observed in brains of PD patients (26). MPTP selectively lesions dopaminergic neurons in the substantia nigra (SN) in mice. It thereby reduces dopamine contents predominantly in the striatum but also in the hippocampus , which is partly innervated by dopaminergic fibers from the SN (27, 28). The dopamine depletion not only leads to motor symptoms comparable to those seen in PD patients but also to impairments of hippocampus-dependent learning and memory functions (29).

For lesioning, mice from study 1 received three intraperitoneal injections of MPTP-HCl dissolved in 0.9% NaCl at a dose of 20 mg/kg bodyweight every 24 h. Control animals were injected with 0.9% NaCl instead.

2.3.2 Diet-induced obesity mouse model

Obesity was induced by feeding mice from study 3 a HFD offering 5.24 kcal/g (60% fat, 20% protein, and 20% carbohydrates) for twelve weeks. Control animals received a control diet of normal calorie content of 3.85 kcal/g (10% fat, 20% protein, and 70% carbohydrates). The daily

amount of ingested food and weekly body weight were monitored. A detailed list of the diets' ingredients is given in the supplementary material (supplementary table1) in (25).

2.4. Behavioral testing: Morris water maze

To assess spatial learning and memory abilities, mice from study 2 and 3 were tested in the MWM. A modified reversal learning protocol was applied as described elsewhere (30). Briefly, mice were trained over three consecutive days (acquisition phase) to locate a platform hidden 1 cm below the water surface in a circular pool. The water was made opaque with milk and its temperature kept at 20°C ± 1°C. In support of spatial memory formation of the platform location, visual cues were placed in each corner of the testing chamber. Each day consisted of six trials during which each mouse was allowed to search for up to 120 s for the platform. Mice were released from varying starting positions. In order to test for flexible memory expression, defined as the ability to use previously learned information in a novel situation (31), the platform was relocated into the opposite quadrant on day 4 and kept there for two days in total (reversal phase). Behavior was automatically tracked using the Viewer 3 software (Biobserve). Spatial learning and memory abilities were determined by analyzing the latency and distance swam to reach the platform, the time spent in the different quadrants, and the number of previous target zone crossings. In study 2, additional classification and analysis of search strategies were performed by analyzing the recorded xy-coordinates using an algorithm previously introduced (30) to investigate qualitative properties of learning in the MWM.

2.5 Magnetic resonance elastography

MRE was performed on a 7 T MRI scanner. During measurements, mice were under inhalational isoflurane/oxygen anesthesia with respiration being automatically monitored. As described elsewhere (20), mouse brains were mechanically stimulated by transmitting vibrations through a tooth-bar onto the scull. 900 Hz external mechanical vibrations were induced by air-cooled Lorentz coils and recorded by FLASH sequence equipped with motion sensitizing gradients (MSG). One transverse 2 mm thick slice was acquired. Further imaging parameters were: 128x128 matrix, 25 mm FoV, 14.3 ms echo time, 116.2 ms repetition time, 285 mT/m MSG strength, eight dynamic scans over a vibration period. Algebraic Helmholtz inversion was performed on 2D complex wave images. This yielded the complex shear modulus G*, which was spatially averaged over two regions of interest, the whole brain parenchyma and the hippocampal area. This was manually segmented by delineating its anatomical structure from MRE magnitude images (Figure 1). The real part of G*, $G'=Re(G^*)$, reflects tissue elasticity. The imaginary part of G*, $G''=Im(G^*)$, relates to

viscosity, which is determined by the density and geometry of the mechanical network in biological tissues. In materials with dominating elastic behavior, the magnitude $|G^*| = abs(G^*)$ and the loss tangent $\varphi = arctan(G''/G')$ represent similar properties as G' and G''. However, in highly crosslinked biological tissues, the phase angle φ better represents geometrical changes in the mechanical network than G'' (32). In general, an increase of these parameters reflects tissue stiffening, while a decrease reflects tissue softening.
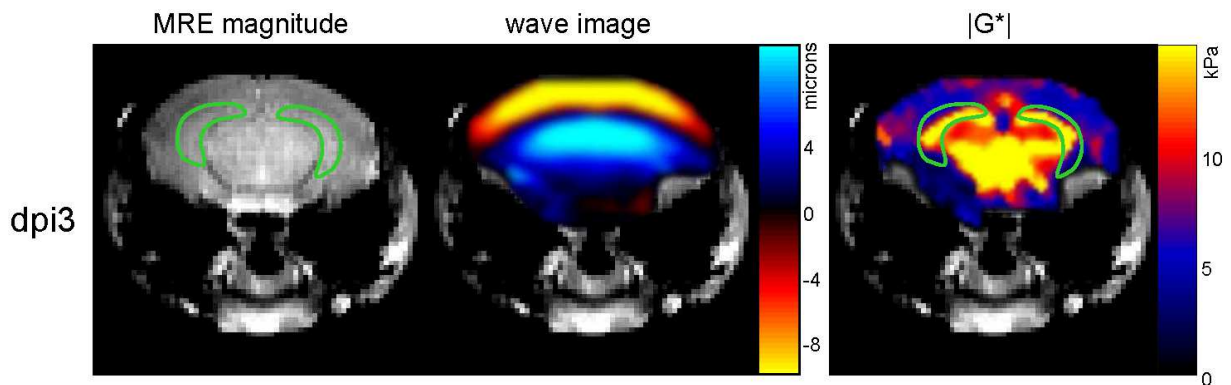
Figure 1: Representative images of the magnitude MRE signal, shear waves and the magnitude complex modulus $|G^*|$ in a mouse. The green line demarcates the chosen region of interest in the hippocampus (from 22).

2.6 Histology and cell quantification

2.6.1 Immunohistochemistry

To quantify the number of newborn (proliferating) cells, immature neurons and microglia and macrophages in the DG of the hippocampus, separate one-in-twelve (study 1 and 3) or one-in-six series (study 2) of free-floating brain sections were stained for BrdU-, DCX- and Iba1-detection as described previously (10, 33). Briefly, after pretreatment with H_2O_2 and HCl (the latter only for BrdU-detection), sections were blocked with PBS+ (0.1% Triton, 3% donkey serum) before being incubated overnight with diluted primary antibodies. The next day, sections were incubated with diluted biotinylated secondary antibodies followed by ABC reagent before visualization by 3,3'-Diaminobenzidine (DAB)-NiCl staining. DAB-stained cells were counted in four or eight brain sections, respectively, under 400x magnification of a light microscope and multiplied by twelve (study 1 and 3) or six (study 2), respectively, to obtain the estimated absolute numbers per hippocampus.

2.6.2 Immunofluorescence

To determine the phenotypes of the newborn cells in the DG, one-in-twelve series of free-floating brain sections were double- or triple-labeled with BrdU, GFP for Nestin-staining, DCX, the mature neuron marker neuronal nuclei (NeuN), and the astrocyte marker glial fibrillary acidic protein (GFAP). After DNA denaturation with HCl, which was required for BrdU staining, the brain sections were blocked with PBS+ and then incubated overnight with the diluted primary antibodies. The next day, sections were incubated with the diluted fluorescent secondary antibodies Rhodamine X, Alexa 488 and Alexa 647. To detect co-labeled cells in the BrdU/Nestin-GFP/NeuN (study 1), BrdU/NeuN (study 2 and 3), and BrdU/Nestin-GFP/GFAP and BrdU/Nestin-GFP/DCX (study 2) stainings, 50 BrdU-positive cells spread across the rostrocaudal extent of the DG in four brain sections were randomly selected and sequentially scanned (z-stacks) using a confocal microscope. The obtained ratios of the different cellular phenotypes were used to determine their estimated absolute numbers per hippocampus.

2.7 Enzyme-linked immunosorbent assay

Hippocampal BDNF protein levels were measured using a commercial ELISA kit. The hippocampus was dissected from fresh-frozen brain tissue taken from mice from study 3 (behavioral group) and ultrasonically homogenized in extraction buffer. After centrifugation, the supernatant was diluted 1:10. The ELISA was principally performed according to the manufacturer's instructions but improved and modified according to the fluorometric technique (34).

2.8 Statistical analyses

Statistical analysis was performed in SPSS Statistics 19 and 21. Graphical presentation of the data was done in GraphPad Prism 5.0. One-way ANOVA, two-way ANOVA, repeated measures ANOVA or chi-square-independence test was applied depending on the analyzed variable. For post-hoc group comparison, Bonferroni or Tamhane's T2 test was used where appropriate. The level of significance was set at $p < 0.05$.

Table 1: List of all substances used in the experiments and analysis including dilution and dose applied.

Substance	Abbreviation	Dilution/Dose	Company
1-Methyl-4-phenyl-1,2,3,6-tetrahydropyridine Hydrochloride	MPTP-HCl	10 mg/ml, 20 mg/kg BW	Sigma-Aldrich
High-fat diet (D12492), 60% fat	HFD	5.24 kcal/g	Research Diets Inc.
Control diet (D12459), 10% fat	CD	3.85 kcal/g	Research Diets Inc.
5'-Bromo-2'-deoxyuridine	BrdU	10 mg/ml, 50 mg/kg BW	Sigma-Aldrich
Brain-derived neurotrophic factor ELISA kit	BDNF ELISA		Promega Inc.
5'-Bromo-2'-deoxyuridine antibody rat	anti-BrdU	1:500	AbD Serotex
Green-fluorescent protein antibody rabbit	anti-GFP rb	1:250	Abcam
Green-fluorescent protein antibody chicken	anti-GFP ck	1:250	Novus Biologicals
doublecortin antibody goat	anti-DCX gt	1:200	Santa-Cruz
Neuronal nuclei antibody mouse	anti-NeuN ms	1:100	Millipore
Glial fibrillary acidic protein antibody goat	anti-GFAP gt	1:200	Santa-Cruz
Biotin rat, goat, rabbit		1:250	Dianova
Rhodamine X rat		1:250	Dianova
Alexa 488 rabbit, chicken, mouse		1:1000	Invitrogen
Alexa 647 mouse		1:300	Dianova
Alexa 647 goat		1:100	Invitrogen
Ionized calcium-binding adaptor molecule 1 antibody rabbit	anti-Iba1 rb	1:1000	Wako
Vectastain® ABC Elite kit	ABC reagent	9 µl/ml	Vector Laboratories
3,3'-Diaminobenzidine	DAB	0.025 mg/ml	Sigma-Aldrich
2-methylbutane	$C_{15}H_{12}$	undiluted	Sigma-Aldrich
Nickelchloride	Ni_2Cl	0.4 mg/ml	Sigma-Aldrich
Paraformaldehyde	PFA	40 g/l	Sigma-Aldrich
Phosphate-buffered saline	PBS		Roth
Sucrose	$C_{12}H_{22}O_{11}$	30 g/ml	Roth
Triton X-100 10%	Triton	10 ml/l	Fluka
Hydrogen peroxide 30%	H_2O_2	20 ml/l	Roth
Hydrochloride acid	HCl	2 M	Merck
Ketamine hydrochloride 10%	Ketamine	0.75 ml/25 g BW	WDT
Xylacine (Rompun) 2%	Xylacine	0.25 ml/25 g BW	Provet AG

3. Results

3.1 Study 1: Enhanced adult neurogenesis increases brain stiffness in a mouse model of dopamine depletion

MRE was performed one day prior to MPTP treatment to obtain baseline data, and 3, 6, 10, 14, and 18 days after treatment to determine viscoelastic alterations as a consequence of MPTP-induced dopamine depletion in the hippocampus that contains the highly neurogenic SGZ. Viscoelastic parameters G′, G″ and abs(G*) were transiently increased in the hippocampal region (G′: $F_{(5,40)}$ = 5.239, p<0.001; G″: $F_{(5,40)}$ = 9.699, p<0.001; abs(G*): $F_{(5,40)}$ = 5.689, p<0.001). MPTP treatment specifically provoked a brain tissue stiffening at 6 dpi (p<0.01). Mean values (± S.E.M.) in the hippocampus of MPTP-treated mice were 6.971 (1.019) kPa, 1.767 (0.103) kPa, and 8.192 (1.011)

kPa for G′, G″ and abs(G*) compared to 4.608 (0.719) kPa, 1.388 (0.125) kPa, and 4.816 (0.705) kPa for G′, G″ and abs(G*) in controls. Similar control values were found for the entire brain parenchyma: 5.234 (0.564) kPa, 1.447 (0.87) kPa, and 5.432 (0.553) kPa for G′, G″ and abs(G*). Relative to baseline values, the changes of G′, G″ and abs(G*) at 6 dpi in the hippocampus of MPTP-treated mice were 51%, 27%, and 49%, and 29%, 16%, and 28% in the whole brain. The phase angle φ remained unchanged by treatment during the course of measurements, which suggests that the viscoelasticity of hippocampal tissue is selectively altered after MPTP treatment without affecting the architecture of the cellular matrix.

Adult neurogenesis in the hippocampus, as a robust correlate of neuronal plasticity likely regulated by the neurotransmitter dopamine, was evaluated by labeling proliferating cells through injecting the mitotic marker BrdU, which is incorporated into the replicating DNA after cell division. MPTP-induced dopamine depletion transiently increased the number of newly generated neural precursor cells and new neurons relative to the number of BrdU-positive cells (BrdU/Nestin-GFP-positive cells: $F_{(5,48)}$ = 9.070, $p<0.0001$; BrdU/NeuN-positive cells: $F_{(5,48)}$ = 41.910, $p<0.0001$). Compared to controls, mice treated with MPTP displayed a larger proportion of new precursor cells at 3 dpi ($p<0.05$) with a subsequent drop at 6 dpi ($p<0.01$, compared to MPTP at 3 dpi) that may suggest a transient reactive proliferation of neural precursor cells in response to the neurotoxin as shown before (Lesemann et al., 2012; Klaissle et al., 2012). In contrast, the proportion of new neurons was elevated at 6 dpi ($p<0.05$) matching the MPTP-induced increase of viscoelastic parameters also found at 6 dpi. Additionally, an increase over time of microglia and macrophages in the DG region could be observed ($F_{(5,48)}$ = 9.635, $p<0.0001$). MPTP treatment provoked elevated numbers of microglia and macrophages specifically at 3 dpi (Iba1: $p<0.05$) compared to healthy controls but did not affect the total number of cells in the granular cell layer of the DG.

3.2 Study 2: Indirect exposure to environmental enrichment is insufficient for enhancing learning and memory and the survival of new neurons in the hippocampus

To investigate, whether indirect exposure to sights, sounds and odors of other mice experiencing the enriched environment is sufficient for enhancing hippocampal neurogenesis and spatial learning and memory function, mice were either directly or indirectly exposed to environmental enrichment for four or eight weeks. No difference in learning abilities between the four groups could be observed. This was indicated by the number of crossings through the previous target area during the first trial on day 4 when the platform position had been relocated to the opposite quadrant. However, over five days with averaged trials per day, ENR mice covered the shortest distance to the hidden platform ($F_{(3,241)}$ = 10.343, $p<0.001$; ENR vs. CTR: $p<0.05$). In contrast, DIR mice did

not differ in swim path length from the CTR group. However, they experienced the same duration of exposure to the enriched environment as mice from the ENR group. Compared to CTR, IND performed worse in the water maze, because they covered a longer distance to the target (p<0.05). Separate analysis of the acquisition (day 1 to 3) and the reversal phase (day 4 and 5) revealed that the poor performance of IND compared to CTR mice predominantly became apparent during the reversal phase ($F_{(3,242)}$ = 7.549, p<0.0001). IND mice more often used hippocampus-independent non-spatial strategies like thigmotaxis, random search, scanning and chaining compared to all other groups (chi-square (3) = 34.276, p<0.001; IND (53.8%) vs. CTR (43.9%), DIR (42.1%) and ENR (35.4%)). ENR mice chose perseverance less often, the preference for the previous target on day 4, compared to CTR and IND mice (chi-square (21) = 44.782, p<0.01; ENR (6.7%) vs. IND (31.3%), CTR (28.3%) and DIR (15.3%)).

Levels of cell proliferation and survival of newborn neurons in the hippocampus were evaluated by injecting BrdU after 28 days of enriched environment either 24 h (proliferation) or four weeks prior to perfusion (survival). As characteristic for the enriched environment paradigm, direct exposure enhanced the survival of newborn BrdU-positive cells ($F_{(3,25)}$ = 13.809, p<0.001; ENR vs. CTR: p<0.001, DIR vs. CTR: p<0.001). In the IND group, when only indirectly experiencing environmental enrichment, this effect was absent. Likewise, the number of newborn mature neurons was only increased in ENR and DIR mice ($F_{(3,25)}$ = 11.673, p<0.0001; ENR vs. CTR: p<0.001, DIR vs. CTR: p<0.01) but not IND mice. This suggests that indirect exposure to an enriched environment is an inadequate stimulus for adult neurogenesis. Only direct interaction is effective in enhancing the survival of newborn neurons. Cell proliferation and numbers of neural precursor cells did not differ between the four groups. This indicates that the beneficial effects of direct interaction with an enriched environment are in fact due to survival-promoting effects instead of increasing cell proliferation or influencing the subpopulations of neural precursor cells.

3.3. Study 3: Concurrent exercise prevents HFD-induced impairment of flexible memory expression associated with adult neurogenesis in the hippocampus

To investigate whether physical exercise can prevent or reverse HFD-induced effects on hippocampal neurogenesis and spatial learning and memory function, HFD was initiated either in adolescent mice (experiment 1) combined with concurrent exercise (preventive) or in adult mice (experiment 2) with 14 days of subsequent exercise (therapeutic). In experiment 1, physical exercise accelerated spatial learning during the acquisition phase, independently of diet ($F_{(2,56)}$=3.320, p<0.05). This was reflected by exercised animals travelling a shorter distance to reach the hidden platform on day 2 compared to sedentary mice (p<0.01). Flexible memory, tested

by a changed platform position on day 4 and 5 of the MWM, was significantly impaired by HFD initiated during adolescence (experiment 1) ($F_{(1,28)}=5.436$, $p<0.05$). The impairment became particularly evident on day 4, when HFD-fed mice covered a longer distance to reach the platform compared to CD mice ($p<0.01$). Independently of time, diet and physical activity interactively influenced flexible memory performance during the reversal phase. This means that HFD only affected sedentary animals ($p<0.01$), while preventively applied exercise prevented the observed impairment in HFD-fed mice ($p<0.01$). In experiment 2, neither exercise nor diet influenced learning performance during days 1 to 3 or flexible memory on days 4 and 5. Analysis of the time spent in quadrants on day 4 revealed an interaction of diet and physical activity ($F_{(1,28)}=15.396$, $p<0.01$), showing that HFD initiated during adolescence increased the time only in sedentary animals ($p<0.001$), which was prevented by exercise ($p<0.001$). Therapeutically applied exercise in experiment 2 yielded an effect of physical activity ($F_{(3,84)}=5.007$, $p<0.01$). This was reflected in the increased time exercising mice spent in the old target quadrant compared to all other quadrants ($p<0.01$ and $p<0.001$).

Adult neurogenesis was evaluated by quantifying the number of proliferating cells and newborn neurons characterized by the incorporated cell proliferation marker BrdU administered at the beginning of HFD exposure, and by the specific neuronal marker NeuN, which labels neurons of a more matured phenotype. Furthermore, total numbers of immature neurons were quantified by counting DCX-positive cells in the SGZ. In experiment 1, exercise strongly stimulated the survival of proliferating cells ($F_{(1,30)}=21.723$, $p<0.001$) and newborn neurons ($F_{(1,30)}=23.725$, $p<0.001$). In experiment 2, both diet and physical activity influenced the survival of proliferating cells ($F_{(1,27)}=4.595$, $p<0.05$ and $F_{(1,27)}=6.202$, $p<0.05$) and newborn neurons ($F_{(1,27)}=7.964$, $p<0.01$ and $F_{(1,27)}=7.734$, 0.01). HFD initiation in adolescent (experiment 1) but not adult (experiment 2) mice reduced the number of immature neurons ($F_{(1,30)} = 14.034$, $p<0.01$. 14 days of exercise subsequent to HFD (experiment 2) stimulated the number of immature neurons independent of diet ($F_{(1,27)} = 79.624$, $p<0.001$). The neurotrophic factor BDNF is frequently discussed as a potential candidate to mediate the effects of obesity and physical exercise on adult neurogenesis in the hippocampus. However, BDNF protein levels in hippocampal tissue samples, determined using an ELISA kit, were not significantly changed by HFD or exercise in both experiments.

4. Discussion

4.1 Newly generated neurons in the DG of the hippocampus potentially integrate with the mechanical scaffold of brain tissue

In response to the MPTP-induced degeneration of dopaminergic neurons, adult neurogenesis in the hippocampus was transiently enhanced. This was attended by a transient increase of MRE constants in the hippocampal tissue. Remarkably, only a 10% change of the neuronal fraction in newly generated cells elicited an apparent invigoration of the viscoelastic lattice at 6 dpi with 50% increased shear modulus (G′). Furthermore, there was no change in viscoelasticity accompanying the transient rise in new neural precursor cells at 3 dpi. This highlights the sensitivity of the macroscopic shear modulus to the number and type of cells engaged in the mechanical tissue matrix.

The observed increase in the number of proliferating precursor cells is in line with previous findings, which demonstrated an acute and transient rise of BrdU/Nestin-GFP-positive cells in the DG and SN, respectively, shortly after MPTP treatment (10, 33). According to studies on other neurodegenerative processes, this may reflect a reactive proliferation of neural precursor cells that could be interpreted as an endogenous regenerative mechanism of the hippocampus to counteract neuronal injury by keeping the endogenous stem-like cell pool at a stable level (35-38). As the rise in neural precursor cells at 3 dpi is followed by increased relative numbers of new neurons at 6 dpi, MPTP treatment may have provoked an increase in the fraction of the reactively generated precursor cells that differentiated into neurons. This further supports the regenerative potential of the hippocampus. In an additional project using the described MPTP mouse model, potential mechanistic pathways of how dopamine regulates neurogenesis in the hippocampus were analyzed using high-pressure liquid chromatography and quantitative polymerase chain reaction (39).

Apparently, neural Nestin-GFP-positive precursor cells do not alter biomechanical constants of brain tissue until their differentiation into neurons. Hence, their mechanical properties must differ from those in neurons. Indeed, neuronal cells have already been demonstrated to be stiffer than glial cells (40) suggesting that neurons play an important structural role in the brain's mechanical scaffold. The distinct brain stiffening as a result of reactively generated neurons induced by a dopamine deficit is in line with previous observations that brain tissue softened in turn as a consequence of neuronal loss in a murine stroke model (41). This further supports the hypothesis that the neuronal network likely establishes the primary mechanical backbone of the brain: a loss of neuronal support in the viscoelastic lattice of the brain may contribute to the global decrease of G′ and G″ observed in the aging brain and in patients with AD and multiple sclerosis (42, 43, 17, 18).

The present study provides the first indication that newly generated neurons in the DG are involved in the viscoelastic matrix of the brain.

4.2 Indirect exposure to a stimulating enriched environment fails to increase the survival of newly generated neurons or to improve hippocampus-dependent learning and memory

Environmental enrichment provoked beneficial effects on hippocampal neurogenesis and learning and memory performance in the MWM only when experienced directly. It did not do so by merely watching, hearing and smelling other mice living in a stimulus-rich environment. Mice of the ENR group, which lived in the enriched environment with an empty inner cage, performed best in the MWM. They covered the shortest distance to find the hidden platform over five days with averaged trials per day suggesting enhanced learning abilities. Furthermore, ENR mice chose perseverance less often as the search strategy to relocate the new platform position on day 4 than all other groups. This indicates improved flexible memory characterized by using the previous learned information in a novel situation. Accordingly, experiencing environmental enrichment - in line with previous studies (44, 12) - promoted the survival of newly generated neurons in the hippocampus. This implicates that these new neurons contributed to the enhanced spatial learning and memory performance in the MWM. Surprisingly, DIR mice, which also directly experienced the enriched environment for the same duration as ENR mice but with an inhabited inner cage, did not show improvements in learning performance. Instead, their swim path length to the platform was even longer than that of CTR mice. However, the survival of new neurons was likewise increased as in ENR mice. The characteristic beneficial effects of an enriched environment on MWM performance are potentially confounded by be the presence of other mice in the inner cage. Their proximity only separated by a transparent wall thereby prohibiting direct interaction might represent a distracting factor that reduced the positive impact of environmental enrichment on spatial learning and memory. This may in turn also account for the poor MWM performance of IND mice living in the inner cage within the inhabited enriched environment. Compared to CTR mice, IND mice performed worse and covered a longer distance to the hidden platform specifically during the reversal phase (day 4 and 5) when the platform had been relocated to the opposite quadrant. Additionally, they also used hippocampus-independent search strategies more often than all other groups. This suggests an additional aversive effect of being indirectly exposed to environmental enrichment than merely not directly experiencing it. This issue needs to be addressed in future experiments.

It has been discussed that an increased level of physical activity might be the actual neurogenesis-stimulating factor in the enriched environment paradigm (45). Given that no suitable monitoring system is available to measure the mice' motility in the present experimental cage-in-cage set-up,

the degree of activity differences between the four groups remains unknown. Physical exercise has been shown to boost neurogenesis by augmenting the proliferation of neural precursor cells in the hippocampus (46), while environmental enrichment has been demonstrated to primarily enhance the survival of newborn neurons (44). As no stimulated proliferation of precursor cells was found in either of the groups directly or indirectly exposed to the enriched environment, the observed increase of adult neurogenesis in ENR and DIR mice is in fact due to an enhanced survival of newly generated neurons.

4.3 Physical exercise initiated concurrently with HFD in adolescent mice prevented the HFD-induced impairment of flexible memory expression

HFD impaired flexible memory in adult mice only when initiated during adolescence but not during adulthood. This is in line with findings from a previous study (13) suggesting that the early life period is particularly susceptible to the adverse effects of HFD on hippocampal-dependent cognitive functioning. On day 4 of the MWM, when the platform had been relocated to another quadrant, HFD-S mice severely struggled with finding the new platform position. Not only did they cover the longest distance to the new target, they also swam all over the maze with particular preference for the previous target quadrant. This probably indicates a reduced flexibility as well as poor search strategies in HFD-fed mice that precluded them from finding the new platform position as quickly as the other mice. The impairment of flexible memory corresponds with a reduced number of immature DCX-positive neurons in the hippocampus. When HFD-S mice were additionally exposed to concurrent physical exercise, however, they mastered the task of relocating the platform just as well as CD-fed mice, in which exercise did not further "boost" healthy flexible memory performance. The observed prevention of flexible memory impairment by exercise might be due to an increased amount of newly generated more mature neurons in the hippocampus of HFD-R mice. Furthermore, concurrent exercise also accelerated the learning process to locate the hidden platform on day 2 of the acquisition phase in CD- but also HFD-fed mice and increased the survival rate of newborn more mature neurons. This finding further supports the proposed functional role of newly generated neurons in learning a hippocampus-dependent cognitive task (11). Both the improved learning during the acquisition phase and the increased number of new mature neurons following physical exercise may reflect a mechanism to compensate for the impaired flexible memory during the reversal phase and the accompanying reduction of immature neurons. To summarize the present results, alterations in learning and flexible memory expression are accompanied by changes in the number of neuronal cells of different maturation stages. More mature neurons probably play a role in learning performance, while immature neurons are rather

critical for flexible memory. In turn, these neurons are differently affected by HFD. This hypothesis is supported by theoretical models already pointing toward different functions of newborn neurons depending on their maturation stage (47-49). However, this needs to be proven in future studies.

In contrast to human studies (50), acute physical exercise over 14 days in experiment 2 did not improve learning abilities in mice. However, exercise slightly increased the number of newborn NeuN-positive neurons and tripled the number of immature neurons in the hippocampus. This may imply that the few exercise-induced generated neurons are probably not sufficient to exert an effect on learning performance. However, it may also imply that the immature neurons do not yet have functional relevance in learning processes. This underlines the proposed different functional roles of immature and more mature neurons. However, the experimental design of the present study – testing spatial learning and memory in the MWM after 14 days of exercise – did not allow for a detection of the proposed functional significance of these neurons in learning abilities once they are matured. This is because differentiation and maturation of exercise-stimulated newly generated cells into neurons and their functional integration takes about four weeks (51). Compared to the acute exercise intervention in experiment 2, long-term physical exercise in experiment 1 did not increase the number of immature neurons. A potential habituation effect to long-term exercise might have set in, at which the acute induction of neurogenesis ceased thereby returning cell numbers to baseline levels (52).

Emerging evidence suggests that obesity and physical inactivity during childhood are associated with cognitive deficits (53). Further human studies regarding potentially modifiable risk factors for AD concluded that there might be an association between mid-life obesity and an increased risk of dementia (54). Therefore, it is under debate whether obesity during childhood and adolescence increases the risk for developing dementia or AD later in life (55). The findings from the present study provide further evidence in support of this.

4.4 Conclusion

A sedentary lifestyle, characterized by physical inactivity combined with excessive television watching and energy-rich diets, is highly prevalent within western civilization. It is strongly associated with increased morbidity and mortality (56-59). We must exercise caution before extrapolating to human situations, because the human lifestyle is far more complex and involves multiple contributing factors compared to keeping mice in an environmentally enriched or running wheel cage. However, the present results clearly show that (1) direct interaction of the individual with the enriched environment is critical for inducing structural and functional changes in the hippocampus and that (2) physical exercise – by regulating adult hippocampal neurogenesis -

might be a potential therapeutic strategy to prevent cognitive impairment later in life associated with obesity during adolescence. Furthermore, the correlation of biomechanical alterations in brain tissue with histological changes contributes to the validation of possible MRE biomarkers for the diagnosis of neuropathological diseases already in a preclinical state to allow more effective therapeutic strategies.

5. Bibliography

1. Brunner EJ, Mosdol A, Witte DR, Martikainen P, Stafford M, Shipley MJ, Marmot M. 2008. Dietary patterns and 15-y-risks of major coronary events, diabetes, and mortality. Am J clin Nutr 87:1414-1421.

2. Francis H, Stevenson R. 2013. The longer-term impacts of western diet on human cognition and the brain. Appetite 63:119-128.

3. Pillon B, Dubois B, Bonnet AM, Esteguy M, Guimares J, Vigouret JM, Lhermitte F, Agid Y. 1989. Cognitive slowing in Parkinson's disease fails to respond to levodopa treatment: the 15-objects test. Neurology 39:762-768.

4. Hoeglinger GU, Rizk P, Muriel MP, Duyckaerts C, Oertel WH, Caille I, Hirsch EC. 2004. Dopamine depletion impairs precursor cells proliferation in Parkinson disease. Nat Neurosci 7:726-735.

5. Boitard C, Cavaroc A, Sauvant J, Aubert A, Castanon N, Layé S, Ferreira G. 2012. Juvenile, but not adult exposure to high-fat diet impairs relational memory and hippocampal neurogenesis in mice. Hippocampus 22:2095-2100.

6. Schinder AF, Gage FH. 2004. A Hypothesis about the role of adult neurogenesis in hippocampal function. Physiology (Bethesda) 19:253-261.

7. Kempermann G, Jessberger S, Steiner B, Kronenberg G. 2004. Milestones of neuronal development in the adult hippocampus. Trends Neurosci 27:447-452.

8. Bonfanti L, Peretto P. Adult Neurogenesis in mammals – a theme with many variations. 2011. Eur J Neurosci 34:930-950.

9. Kempermann G. 2011. Seven principles in the regulation of adult neurogenesis. Eur J Neurosci 33:1018-1024.

10. Lesemann A, Reinel C, Huehnchen P, Pilhatsch M, Hellweg R, Klaissle P, Winter C, Steiner B. 2012. MPTP-induced hippocampal effects on serotonin, dopamine, neurotrophins, adult neurogenesis and depression-like behavior are partially influenced by fluoxetine in adult mice. Brain Res 1457:51-69.

11. Van Praag H, Christie BR, Sejnowski TJ, Gage FH. 1999. Running enhances neurogenesis, learning, and long-term potenitation in mice. Proc Natl Acad Sci USA 96:13427-13431.

12. Nilsson M, Perfilieva E, Johansson U, Orwar O, Eriksson PS. 1999. Enriched environment increases neurogenesis in the adult rat dentate gyrus and improves spatial memory. J Neurobiol 39:569-578.

13. Boitard C, Cavaroc A, Sauvant J, Aubert A, Castanon N, Layé S, Ferreira G. 2012. Juvenile, but not adult exposure to high-fat diet impairs relational memory and hippocampal neurogenesis in mice. Hippocampus 22:2095-2100.

14. Mu Y, Gage FH. 2011. Adult hippocampal neurogenesis and its role in Alzheimer's disease. Mol Neurodegener 6:85.

15. Barthel H, Mueller U, Waechter T, Slomka P, Dannenberg C, Murai T, Kahn T, Georgi P. 2000. Multimodale SPECT- und MRT-Bilddatenanalyse zur Verbesserung der Diagnostik des idiopathischen Parkinson-Syndroms. Radiologie 40:863-869.

16. McKhann GM, Knopman DS, Chertkow H, Hyman BT, Jack Jr CR, Kawas CH, Klunk WE, Koroshetz WJ, Manly JJ, Mayeux R, Mohs RC, Morris JC, Rossor MN, Scheltens P, Carrillo MC, Thies B, Weintraub S, Phelps CH. 2011. The diagnosis of dementia due to Alzheimer's disease: Recommendations from the National Institute on Aging-Alzheimer's Association workgroups on diagnostic guidelines for Alzheimer's disease. Alzheimers Dement 7:263-269.

17. Wuerfel J, Paul F, Beierbach B, Hamhaber U, Klatt D, Papazoglou S, Zipp F, Martus P, Braun J, Sack I. 2010. MR-elastography reveals degradationof tissue integrity in multiple sclerosis. Neuroimage 49:2520-2525.

18. Streitberger K-J, Sack I, Krefting D, Pfueller C, Braun J, Paul F, Wuerfel J. 2012. Brain viscoelasticity alteration in chronic-progressive multiple sclerosis. PLoS One 7:e29888.

19. Schregel K, Wuerfel neé Tysiak E, Garteiser P, Gemeinhardt I, Prozorovski T, Aktas O, Merz H, Petersen D, Wuerfel J, Sinkus R. 2012: Demyelination reduces brain parenchymal stiffness quantified in vivo by magnetic resonance elastography. Proc Natl Acad Sci U.S.A. 109:6650-6655.

20. Riek K, Millward JM, Hamann I, Mueller S, Pfueller CF, Paul F, Braun J, Infante-Duarte C, Sack I. 2012. Magnetic resonance elastography reveals altered brain viscoelasticity in experimental autoimmune encephalomyelitis. NeuroImage: Clinical 1:81-90.

21. Lendahl U, Zimmermann LB, McKay RDG. 1990. CNS stem cells express a new class of intermediate filament protein. Cell 60:585-595.

22. Klein C, Hain EG, Braun J, Riek K, Mueller S, Steiner B, Sack I. 2014. Enhanced adult neurogenesis increases brain stiffness: *in vivo* magnetic resonance elastography in a mouse model of dopamine depletion. PLoS One:e92582.

23. Morris RGM, Garud P, Rawlins JNP, O'Keefe J. 1982. Place navigation impaired in rats with hippocampal lesions. Nature 297:681-683.

24. Iggena D, Klein C, Garthe A, Winter Y, Kempermann G, Steiner B. 2015. Only watching others making their experiences is insufficient to enhance adult neurogenesis and water maze performance in mice. Sci Rep 5:14141.

25. Klein C, Jonas W, Iggena D, Empl L, Rivalan M, Wiedmer P, Spranger J, Hellweg R, Winter Y, Steiner B. 2016. Neurobiol Learn Mem 131:26-35.

26. Langston JW, Ballard P, Tetrud JW, Irwin I. 1983. Chronic Parkinsonism in humans due to a product of meperidine-analog synthesis. Science 219:979-980.

27. Marsden CD, Jenner PG. 1987. The significane of 1-methyl-4-phenyl-1,2,3,6-tetrahydropyridine. Ciba Found Symp 126:239-256.

28. Scatton B, Simon H, Le Moal M, Bischoff S. 1980. Origin of dopaminergic innervation of the rat hippocampal formation. Neurosci Lett 18:125-131.

29. Deguil J, Chavant F, Lafay-Chebassier C, Pérault-Pochat M-C, Fauconneau B, Pain S. 2010. Neuroprotective effect of PACAP on translational control alteration and cognitive decline in MPTP parkinsonian mice. Neurotox Res 17:142-155.

30. Garthe A, Behr J, Kempermann G. 2009. Adult-generated hippocampal neurons allow the flexible use of spatially precise learning strategies. PLoS One 4:e5464.

31. Dupret D, Revest JM, Koehl M, Ichas F, De Giorgi F, Costet P, Abrous DN, Piazza PV. 2008. Spatial relational memory requires hippocampal adult neurogenesis. PLoS One 3:e1959.

32. Posnansky O, Guo J, Hirsch S, Papazoglu S, Braun J, Sack I. 2012. Fractal network dimension and viscoelastic powerlaw behavior: I. A modeling approach based on a coarse-graining procedure combined with shear oscillatory rheometry. Phys Med Biol 57:4023-4040.

33. Klaissle P, Lesemann A, Huehnchen P, Hermann A, Storch A, Steiner B. 2012. Physical activity and environmental enrichment regulate the generation of neural precursors in the adult mouse subtantia nigra in a dopamine-dependent manner. BMC Neurosci 13:1-15.

34. Hellweg R, von Arnim CA, Bücher M, Huber R, Riepe MW. 2003. Neuroprotection and neuronal dysfunction upon repetitive inhibition of oxidative phosphorylation. Exp Neurol 183:346-354.

35. Aharoni R, Arnon R, Eilam R. 2005. Neurogenesis and neuroprotection induced by peripheral immunomodulatory treatment of experimental autoimmune encephalomyelitis. J Neurosci 25:8217-8228.

36. Arvidsson A, Collin T, Kirik D, Kokaia Z, Lindvall O. 2002. Neuronal replacement from endogenous precursors in the adult brain after stroke. Nat Med 8:963-970.

37. Gage FH, Kempermann G, Palmer TD, Peterson DA, Ray J. 1998. Multipotent progenitor cells in the adult dentate gyrus. J Neurobiol 36:249-266.

38. Huehnchen P, Pozorovski T, Klaissle P, Lesemann A, Ingwersen J, Wolf SA, Kupsch A, Aktas O, Steiner B. 2011. Moldulation of adult hippocampal neurogenesis during myelin-directed autoimmune neuroinflammation. Glia 50:132-142.

39. Klein C, Rasinska J, Empl L, Sparenberg M, Poshtiban A, Hain EG, Iggena D, Rivalan M, Winter Y, Steiner B. Physical exercise counteracts MPTP-induced changes in neural precursor cell proliferation in the hippocampus and restores spatial learning but not memory performance in the water maze. Behav Brain Res (in press).

40. Lu Y-B, Franze K, Seifert G, Steinhaeuser C, Kirchhoff F, Wolburg H, Guck J, Janmey P, Wei E-Q, Käs J, Reichenbach A. 2006. Viscoelastic properties of individual glial cells and neurons in the CNS. Proc Natl Acad Sci U.S.A. 103:17759-17764.

41. Freimann FB, Mueller S, Streitberger K-J, Guo J, Rot S, Ghori A, Vajkoczy P, Reiter R, Sack I, Braun J. 2013. MR elastography in a murine stroke model reveals correlation of macroscopic viscoelastic properties of the brain with neuronal density. NMR Biomed 26:1534-1539.

42. Sack I, Streitberger K-J, Krefting D, Paul F, Braun J. 2011. The influence of physiological aging and atrophy on brain viscoelastic properties in humans. PLoS One 6:e23451.

43. Murphy MC, Huston III J, Jack Jr CR, Glaser KJ, Manduca A, Felmlee JP, Ehman RL. 2011. Decreased brain stiffness in Alzheimer's disease determined by magnetic resonance elastography. J Magn Reson Imaging 34:494-498.

44. Kempermann G, Kuhn HG, Gage FH. 1997. More hippocampal neurons in adult mice living in an enriched environment. Nature 386:493-495.

45. Mustroph ML, Chen S, Desai SC, Cay EB, DeYoung EK, Rhodes JS. 2012. Aerobic exercise is the critical variable in an enriched environment that increases hippocampal neurogenesis and water maze learning in male C57Bl/6 mice. Neuroscience 219:62-71.

46. Van Praag H, Kempermann G, Gage FH. 1999. Running increases cell proliferation and neurogenesis in the adult mouse dentate gyrus. Nature Neurosci 2:266-270.

47. Aimone JB, Wiles J, Gage FH. 2006. Potential role for adult neurogenesis in the encoding of time in new memories. Nat Neurosci 9:723-727.

48. Aimone JB, Wiles J, Gage FH. 2009. Computational influence of adult neurogenesis on memory encoding. Neuron 61:187-202.

49. Deng W, Aimone JB, Gage FH. 2010. New neurons and new memories: how does adult hippocampal neurogenesis affect learning and memory? Nat Rev Neurosci 11:339-350.

50. Kirk-Sanchez NJ, McGough EL. 2014. Physical exercise and cognitive performance in the elderly: current perspectives. Clin Interv Aging 9:51-62.

51. Ehninger D, Kempermann G. 2008. Neurogenesis in the adult hippocampus. Cell Tissue Res 331:243-250.

52. Kronenberg G, Bick-Sander A, Bunk E, Wolf C, Ehninger D, Kempermann G. 2006. Physical exercise prevents age-related decline in precursor cell activity in the mouse dentate gyrus. Neurobiol Aging 27:1505-1513.

53. Burkhalter TM, Hillman CH. 2011. A narrative review of physical activity, nutrition, and obesity to cognition and scholastic performance across the human lifespan. Adv Nutr 2:201S-206S.

54. Barnes DE, Yaffe K. 2011. The projected effect of risk factor reduction on Alzheimer's disease prevalence. Lancet Neurol 10:819-828.

55. Luchsinger JA, Mayeux R. 2007. Adiposity and Alzheimer's disease. Curr Alzheimer Res4:127-134.

56. Kim Y, Wilkens LR, Park SY, Goodman MT, Monroe KR, Kolonel LN. 2013. Association between various sedentary behaviors and all-cause, cardiovascular disease and cancer mortality: the Multoethnic Cohort Study. Int J Epidemiol 41:1040-1056.

57. Wilmot EG, Edwadrson CL, Achana FA, Davies MJ, Gorely T, Gray LJ, Khunti K, Yates T, Biddle SJ. 2012. Sedentary time in adults and association with diabetes, cardiovascular disease and death: systematic review and meta-analysis. Diabetologica 55:2895-2905.

58. Sund AM, Larsson B, Wichstrøm L. 2011. Role of physical and sedentary activities in the development of depressive symptoms in early adolescence. Soc Psychiatry Psychiatr Epidemiol 46:431-441.

59. Lindstrom HA, Fritsch T, Petot G, Smyth KA, Chen CH, Debanne SM, Lerner AJ, Friedland RP. 2005. The relationship between television viewing in midlife and the development of Alzheimer's disease in a case-control study. Brain Cogn 58:157-165.

Affidavit

I, Charlotte Klein, certify under penalty of perjury by my own signature that I have submitted the thesis on the topic "Effects of physical activity and nutrition on neuronal plasticity, neurogenesis and cognition in the healthy brain and in a mouse model of Parkinson's disease". I wrote this thesis independently and without assistance from third parties, I used no other aids than the listed sources and resources.

All points based literally or in spirit on publications or presentations of other authors are, as such, in proper citations (see "uniform requirements for manuscripts (URM)" the ICMJE www.icmje.org) indicated. The sections on methodology (in particular practical work, laboratory requirements, statistical processing) and results (in particular images, graphics and tables) correspond to the URM (s.o) and are answered by me. My contributions in the selected publications for this dissertation correspond to those that are specified in the following joint declaration with the responsible person and supervisor. All publications resulting from this thesis and which I am author of correspond to the URM (see above) and I am solely responsible.

The importance of this affidavit and the criminal consequences of a false affidavit (section 156,161 of the Criminal Code) are known to me and I understand the rights and responsibilities stated therein.

_____   _____

Date   Signature

Declaration of any eventual publications

Charlotte Klein had the following share in the following publications:

Publication 1:
Klein C, Hain EG, Braun J, Riek K, Mueller S, Steiner B, Sack I. 2014. Enhanced adult neurogenesis increases brain stiffness: *In vivo* magnetic resonance elastography in a mouse model of dopamine depletion. *PLoS ONE.*
IF: 3.5 (2013/2014)

Contribution in detail: 80%. Partly conceived and designed the study, performed experiments including animal handling, injections, MRE measurements, brain tissue processing, and histological staining and counting, analyzed the data, wrote the manuscript and corresponded with the editor/reviewer.

Publication 2:

Iggena D, **Klein C**, Garthe A, Winter Y, Kempermann G, Steiner B. 2015. Only watching others making their experiences is insufficient to enhance adult neurogenesis and water maze performance in mice. *Sci Rep.*

IF: 5.6 (2014/2015)

Contribution in detail: 20%. Partly performed experiments including animal handling, injections, and behavioral experiments and revised the manuscript.

Publication 3:

Klein C, Jonas W, Iggena D, Empl L, Rivalan M, Wiedmer P, Spranger J, Hellweg R, Winter Y, Steiner B. In print. Exercise prevents high-fat diet-induced impairment of flexible memory expression in the water maze and modulates adult hippocampal neurogenesis in mice. *Neurobiol Learn Mem.*

IF: 3.7 (2014/2015)

Contribution in detail: 80%. Performed experiments including animal handling, injections, behavioral testing, brain tissue processing, and histological staining and counting, analyzed the data, wrote the manuscript and corresponded with the editor/reviewer.

Signature, date and stamp of the supervising University teacher

_____

Signature of the doctoral candidate

_____

PLOS ONE

Enhanced Adult Neurogenesis Increases Brain Stiffness: *In Vivo* Magnetic Resonance Elastography in a Mouse Model of Dopamine Depletion

Charlotte Klein[1], Elisabeth G. Hain[1], Juergen Braun[2], Kerstin Riek[3], Susanne Mueller[4], Barbara Steiner[1]*⁹, Ingolf Sack[3]⁹

1 Department of Neurology, Charité - University Medicine Berlin, Berlin, Germany, 2 Institute of Medical Informatics, Charité - University Medicine Berlin, Berlin, Germany, 3 Department of Radiology, Charité - University Medicine Berlin, Berlin, Germany, 4 Center for Stroke Research Berlin, Berlin, Germany

Abstract

The mechanical network of the brain is a major contributor to neural health and has been recognized by in vivo magnetic resonance elastography (MRE) to be highly responsive to diseases. However, until now only brain softening was observed and no mechanism was known that reverses the common decrement of neural elasticity during aging or disease. We used MRE in the 1-methyl-4-phenyl-1,2,3,6-tetrahydropyridine hydrochloride (MPTP) mouse model for dopaminergic neurodegeneration as observed in Parkinson's disease (PD) to study the mechanical response of the brain on adult hippocampal neurogenesis as a robust correlate of neuronal plasticity in healthy and injured brain. We observed a steep transient rise in elasticity within the hippocampal region of up to over 50% six days after MPTP treatment correlating with increased neuronal density in the dentate gyrus, which could not be detected in healthy controls. Our results provide the first indication that new neurons reactively generated following neurodegeneration substantially contribute to the mechanical scaffold of the brain. Diagnostic neuroimaging may thus target on regions of the brain displaying symptomatically elevated elasticity values for the detection of neuronal plasticity following neurodegeneration.

Competing Interests: The authors have declared that no competing interests exist.

* E-mail: barbara.steiner@charite.de

⁹ These authors contributed equally to this work.

Introduction

Magnetic resonance elastography (MRE) has been developed over the last few years as a non-invasive tool to evaluate the elasticity of biological tissues [1]. The presence of the skull has always prevented manual palpation of the brain, but MRE now offers the possibility to assess brain consistency under physiological and pathological conditions by in-vivo imaging [2–7]. In the brain, the viscoelastic properties are determined by neurons, glial cells [8] and extracellular matrix in addition to fluid flow of interstitial fluid, CSF and blood [9]. Disruption of this complex system by pathological processes provokes mechanical responses, which are influential to the progression of the disease but also of potential value for its diagnosis and clinical assessment. However, the biophysical mechanisms behind an alteration of the mechanical properties of tissue are entirely unknown in the brain.

It has just recently been discovered that brain elasticity is reduced in the course of physiological aging [10] and in diseases such as normal pressure hydrocephalus (NPH) [11], Alzheimer's disease (AD) [12] and multiple sclerosis (MS) [13,14]. First steps to correlate these findings with the histopathology have been taken quite recently by Schregel and colleagues inducing reversible toxic demyelination in the mouse [15] and by Riek and co-workers who studied the effect of inflammation in a mouse model of experimental autoimmune encephalitis (EAE) [16]. Both groups observed a marked decrease of viscoelastic constants similar to what has been detected in patients with NPH, AD and MS. Of particular interest is a very recent study by Freimann and co-workers demonstrating a clear correlation of brain tissue softening with reduced neuronal density after middle cerebral artery occlusion (MCAO) in mice, which is a commonly used stroke model [17]. It is remarkable that all pathophysiological processes studied by cerebral MRE so far exhibited a rather unspecific reduction in either elasticity or viscosity or both. Inversely, no neural alteration has been observed associated with an increase of viscoelastic constants. Potentially, such a disease-related process would appear highly significant in diagnostic MRE since it would be distinguishable from the general pattern of tissue softening reported in the literature. Based on previous work that showed the correlation between neuronal density and macroscopic brain stiffness by inducing neuronal loss [17], we hypothesize that the generation of new neurons would increase the macroscopic elasticity of the brain. Given that this hypothesis is corroborated, our study would provide an indication about the close relationship between brain mechanical constants and neuronal network density.

The generation of new neurons should be apparent in regions with high cellular turnover. In the adult brain, new nerve cells are

generated in the subgranular zone (SGZ) of the hippocampal dentate gyrus (DG) at substantial levels throughout lifetime. Here, neural precursor cells characterized by the expression of the intermediate filament nestin [18] continuously proliferate and mature into functionally integrated cells in the granular cell layer (GCL) via a multistep process termed adult neurogenesis [19–21]. It has been shown that a homeostasis of neurotransmitters such as dopamine plays a key role in the regulation of adult neurogenesis and the maintenance of a so-called neurogenic niche. Alterations in dopamine levels as observed in Parkinson's disease (PD) and its animal models result in significant quantitative changes of newly generated neural precursor cells and mature neurons in the DG [22–30].

Therefore, we applied MRE to such a mouse model of dopamine depletion, which is induced by the neurotoxin 1-methyl-4-phenyl-1,2,3,6-tetrahydropyridine hydrochloride (MPTP) leading to degeneration of dopaminergic neurons in the substantia nigra pars compacta (SNpc) with a subsequent dopamine deficit in the striatum, hippocampus and other brain areas that are innervated by dopaminergic fibers from the SNpc [31–35]. Cellular changes in the DG of the hippocampus as a consequence of the induced dopamine deficit were visualized by labelling newly generated cells in the SGZ with specific mitotic and neuronal markers, and characterized and quantified using confocal microscopy. To also determine alterations in the total cell number, cells of the GCL in the DG including the SGZ were counted using stereological microscopy. Hence, this animal model of dopamine depletion provides the possibility to examine how alterations of the neuronal matrix in certain brain areas resulting from a dopamine deficit relate to MRE measurements, and to expand the utility of MRE as a tool to monitor cellular changes in the pathology of neurodegenerative diseases.

Materials and Methods

Animals

A total of 60 eight to ten weeks old female transgenic C57Bl/6 mice (Forschungseinrichtung für experimentelle Medizin, FEM, Berlin, Germany), expressing the green fluorescent protein (GFP) under the nestin promoter, were group-housed (n = 5) in a temperature- and humidity-controlled colony room and maintained on a light/dark cycle of 12/12 h (lights on at 6 am) with ad libitum access to rodent lab chow and water. All experiments were approved by the local animal ethics committee (Landesamt für Gesundheit und Soziales, Berlin) and were carried out in accordance with the European Communities Council Directive of 24 November 1986 (86/609/EEC).

Group Design and Experimental Procedure

The mice were randomly assigned to four groups in total - three for histology and one for MRE. The MRE group (n = 5) was investigated first without any modifications for obtaining reference (baseline) data; then MRE was applied at five time-points after NaCl treatment at 3, 6, 10, 14 and 18 days post injection (dpi), followed by MPTP treatment and MRE measurements again at 3, 6, 10, 14 and 18 dpi. The last MRE measurement of NaCl-treated mice (18 dpi) also served as baseline data of MPTP-treated mice.

The histology groups (not investigated by MRE) comprised untreated mice (baseline; n = 5) and treated animals either with MPTP (MPTP; n = 25) or with NaCl (Control, CTR; n = 25). The treated groups (MPTP and CTR) were further subdivided into groups of five, which were sacrificed at 3, 6, 10, 14 and 18 days after the MPTP/NaCl treatment period. Figure 1a summarizes the timeline of the injections, MRE experiments and histology.

MPTP Model

1-methyl-4-phenyl-1,2,3,6-tetrahydropyridine hydrochloride (MPTP, Sigma-Aldrich, Steinheim, Germany) was dissolved in 0.9% NaCl.

For lesioning, a protocol previously applied was followed [27,28]. Briefly, mice received three single intraperitoneal (i.p.) injections of MPTP (20 mg/kg body weight; in total 60 mg/kg) on three consecutive days every 24 hours. Control animals were treated with injections of 0.9% NaCl instead for the same time period. Control mice of the baseline group remained untreated.
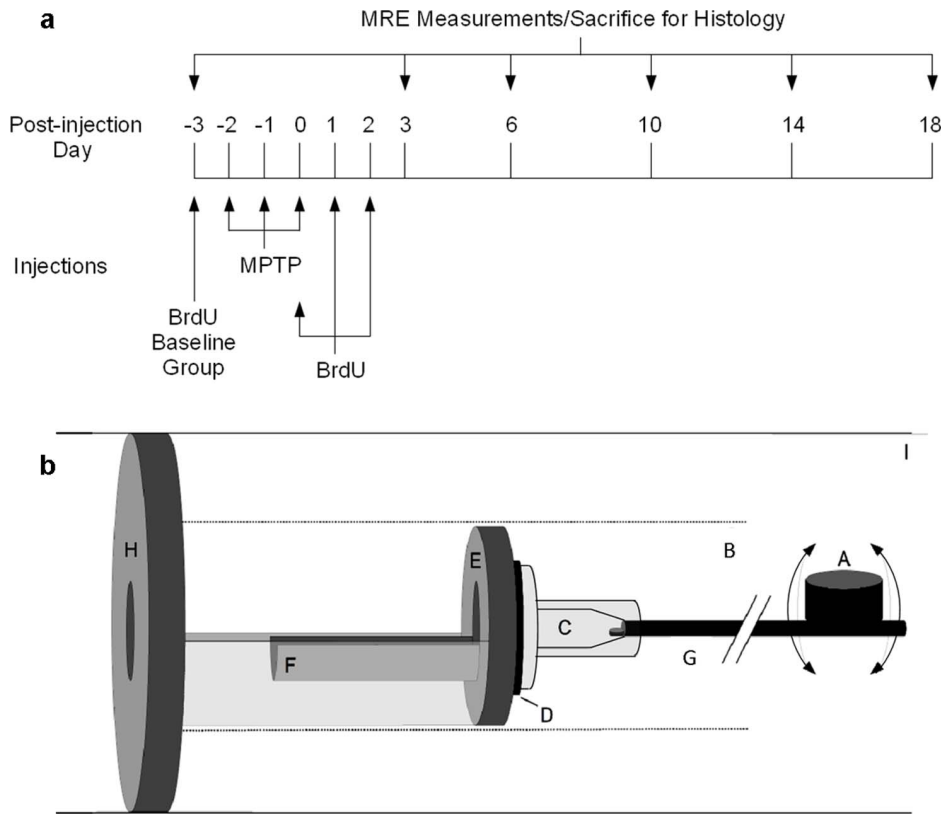
BrdU Injections

Bromodesoxyuridine (BrdU, Sigma-Aldrich, Steinheim, Germany), used here as the mitotic marker to label proliferating cells, was dissolved in 0.9% NaCl and filtered. Animals received three single i.p. injections of BrdU (50 mg/kg body weight; in total 150 mg/kg) on three consecutive days every 24 h. BrdU treatment started at the final day of MPTP-injections.

Magnetic Resonance Elastography (MRE)

Mechanical stimulation. Mouse brains were mechanically stimulated as previously illustrated [16]. A schematic of the experimental setup is shown in Figure 1b. Briefly, the vibration source was an electromagnetic coil, attached to a carbon fiber piston, the end of which was mounted to the respiratory mask with a bite-bar transducer. The transducer was gimballed through a rubber bearing and retaining bracket at the temperature-controlled mouse bed. The entire setup was held in the centre of the magnet bore by a plastic disk. Vibrations were produced by applying a sinusoidal current of 900 Hz frequency to an air-cooled Lorentz coil in the fringe field of the MRI scanner. Frequency amplitude and number of sinusoidal oscillation cycles were controlled by an arbitrary function generator connected via an audio amplifier to the driving coil. The main polarization of the vibration was transverse to the principal axis of the magnet field, with amplitudes in the order of tens of micrometers.

Data acquisition and analysis. As previously described [16,17], all measurements were performed on a 7 tesla scanner (Bruker PharmaScan 70/16, Ettlingen, Germany) running Para-Vision 4.0 software and using a 20 mm diameter 1H-RF-quadratur mouse head volumecoil. The vibration was initiated by a trigger pulse from the control unit of the scanner, the timing of which was defined by a customized FLASH sequence. The imaging sequence was modified for MRE by sinusoidal motion sensitizing gradient (MSG) in the through-plane direction, as described elsewhere [16]. The MSG strength was 285 mT/m with a frequency of 900 Hz and 9 periods. To compensate for static phase contributions, phase difference images were calculated from two images differing in the sign of the MSG. Further imaging parameters were: a 128×128 matrix, 25 mm FoV, 14.3 ms echo time (TE), 116.2 ms repetition time (TR), eight dynamic scans over a vibration period, one transverse 2-mm slice, and an acquisition time of 20 min.

Complex wave images (Figure 2) corresponding to the harmonic drive frequency were calculated by temporal Fourier transformation of the unfolded phase-difference images and filtered for suppressing noise and compression wave components [16,36]. The pre-processed 2D scalar wave fields were analyzed for the complex shear modulus G* by algebraic Helmholtz inversion [37]. Then, G* was spatially averaged over two regions of interest (ROI's), i) the whole brain parenchyma displayed in the image and ii) the hippocampal area (Figure 2), manually segmented by delineating its anatomical structure from MRE magnitude images. The tabulated spatially averaged G*-values are represented by the real

Figure 1. Timeline of the study design and schematic of the mouse MRE apparatus. The timeline (a) of MPTP and BrdU injections, time-points of MRE measurement and sacrifice for histology. A schematic (b) of the mouse MRE apparatus: (A) driving coil, (B) magnet bore, (C) respiratory mask, (D) rubber bearing, (E) retaining bracket, (F) mouse bed, (G) carbon fiber piston, (H) plastic disk, and (I) Lorentz coil (modified from [16]).
doi:10.1371/journal.pone.0092582.g001

part of the complex shear modulus G*, $G' = Re(G^*)$, known as storage modulus, the imaginary part $G'' = Im(G^*)$, which is the loss modulus, the magnitude $|G^*| = abs(G^*)$ and the loss tangent given by $\varphi = \arctan(G''/G')$. The storage, loss and magnitude moduli are expressed in kilopascals (kPa) while φ is given in radians. In general, G' relates to the elastic properties of a material, while G'' is a measure of viscosity, which is determined by the density and geometry of the mechanical network in biological tissues. In materials with dominating elastic behaviour, the parameters $|G^*|$ and φ represent similar properties as G' and G''. However, in highly crosslinked biological tissues, the phase angle φ better represents geometrical changes in the mechanical network than G'' [38].

Perfusion and Tissue Processing

Mice of the histology groups were sacrificed according to the corresponding MRE measurement time-points as depicted in Figure 1a.

They were deeply anesthetized with an overdose of ketamine (ketamine hydrochloride, 100 mg/ml, WDT) and sacrificed by transcardial perfusion with 1 M phosphate buffered saline (PBS) and 4% paraformaldehyde (PFA). Brains were removed and post-fixed overnight in PFA at 4°C and then transferred into 30% sucrose for dehydration for 48 h. Brains were frozen in 2-methyl butane cooled with liquid nitrogen, cut into 40 µm thick coronal sections (Bregma −0.1 mm to −4.04 mm) using a cryostat (Leica CM 1850 UV) and stored in cryoprotectant-containing 24-well plates at 4°C until histological analysis.

Immunohistochemistry

Immunohistochemistry for the Iba1 antigen as a marker for microglia and macrophages was performed following a well-established staining protocol [28]. Briefly, free-floating 1-in-12 section series were treated with 0.6% H_2O_2 to deactivate endogenous tissue peroxidases. After 30 min background blocking with PBS enriched with 3% donkey serum (PBS+), sections were incubated with primary anti-Iba1 (rabbit, 1:1000, Wako) antibody overnight at 4°C. The next day, after washing with PBS and blocking with PBS+, sections were incubated with biotinylated secondary antibody (anti-rabbit, 1:250, dianova) for 2 h at room temperature (RT). ABC reagent (Vectastatin ABC Elite Kit, Vector Laboratories) was applied for 1 h. Finally, sections were incubated with Diaminobenzidine (DAB)/peroxidase (Sigma, Germany) in a solution containing 0.3% H_2O_2 and 0.01% nickel chloride for at least 5 min at RT. Sections were mounted on microscope slides and coverslipped for later quantification.

Immunofluorescence

For triple-labelling, free-floating 1-in-12 section series were rinsed and incubated as described above except for H_2O_2 pre-treatment but 1 h PBS+ blocking instead. Anti-BrdU (rat, 1:500, AbD Serotex) anti-GFP (chicken, 1:250, Novus Biologicals) and anti-NeuN (mouse, 1:100, Millipore) were used as primary antibodies. BrdU denotes newly generated cells, while BrdU/Nestin (Nestin/GFP) and BrdU/NeuN denote new neural precursor cells and new neurons, respectively. After incubation for 48 h at 4°C, RhodamineX (anti-rat, 1:250, dianova), Alexa 488 (anti-chicken, 1:1000, Invitrogen) and Alexa 647 (anti-mouse,
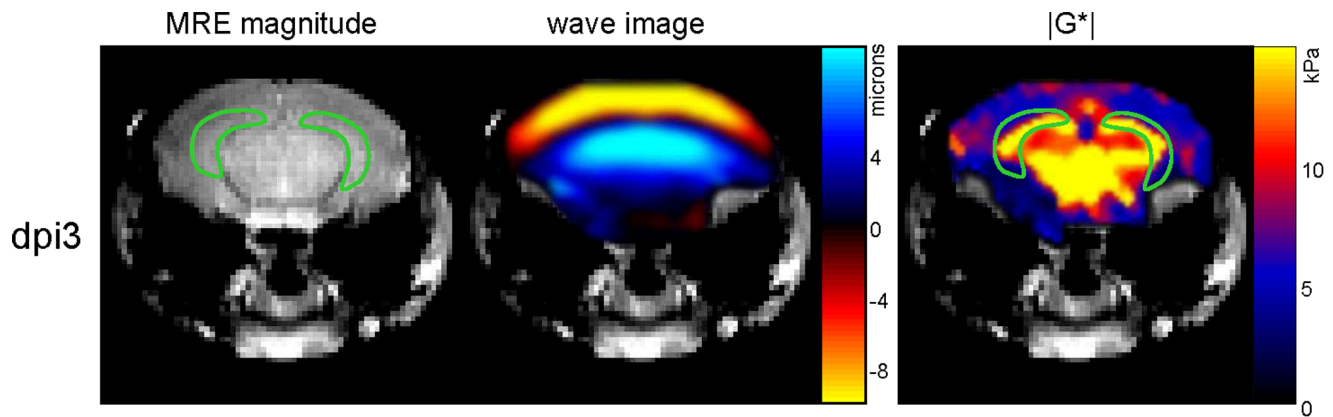
Figure 2. Representative images of the magnitude MRE signal, shear waves and the magnitude complex modulus (|G*|) in a mouse.
The green line demarcates the chosen region of interest in the hippocampus.
doi:10.1371/journal.pone.0092582.g002

1:300, dianova.) as secondary antibodies diluted in PBS+ were applied for 4 h at RT. Sections were mounted on microscope slides and coverslipped for later quantification.

For stereological counting of cells in the GCL of the DG including the cells in the SGZ in order to determine its total cell number, separate 1-in-12 series of sections were incubated with the fluorochrome 4′,6-diamidino-2-phenylindole (DAPI), which binds to the DNA thereby labeling cell nuclei in general. For this purpose, sections were incubated with PBS-diluted DAPI (1:1000, Thermo Scientific) for 7 min and afterwards mounted on microscope slides and coverslipped for later quantification.

Quantification

Iba1-positive cells of DAB/peroxidase-stained 1-in-12 section series (480 μm apart) from all animals were counted throughout the rostrocaudal extent of the GCL/SGZ, molecular layer (ML) and hilus in the hippocampal formation in both hemispheres using the 40×objective of a light microscope (Axioskop, Zeiss, Germany). In total, four brain slices per animal containing the hippocampus were analyzed. Resulting absolute cell numbers were then multiplied by twelve to obtain the estimated total number of Iba1-positive cells per brain.

BrdU-positive cells in the fluorescent-stained sections were counted as described for Iba1 but in the GCL/SGZ only using a fluorescence microscope (Axioskop, Zeiss, Germany).

Double-labeled cells were quantified by analyzing 50 BrdU-positive cells spread throughout the rostrocaudal extent of the GCL/SGZ of four brain slices per animal for co-expression of BrdU and additional markers (Nestin/GFP and NeuN) using a Leica TCS SP2 confocal microscope (400x and 630x amplification). All images were taken in a sequential scanning mode (z-stacks) to identify superposed cell bodies or nuclei, which appeared artificially merged. Then, the percentages of Nestin/GFP- and NeuN-positive cells in all 50 BrdU-cells were determined. These rations along with the total numbers of BrdU-positive cells were then used to calculate the absolute numbers of doubly labeled cells.

For quantification of absolute numbers of DAPI-stained cell nuclei in the GCL, a Leica DMRE microscope and Stereo-Investigator (MicroBrightfield) software were used. The bounderies of the GCL, the region of interest, of five sections per animal were traced at 200×magnification and the thickness of the slices (40 μm) was entered to the software program. The software then randomly arranged counting frames (30 μm×30 μm×30 μm) in a sampling grid (120 μm×100 μm), which was placed over the

region of interest. The DAPI-stained cell nuclei were counted at 400×amplification in oil in the counting frames and in an Optical Disector height of 20 μm, which started 5 μm below the top surface. The total number of cells in the GCL was automatically calculated based on the counted cell number, slice interval, counting frame size, sampling grid size, slice thickness and Optical Disector height.

Statistical Analysis

To test for normal distribution and homogeneous variances, the Kolmogorov-Smirnov test and the Levené test, respectively, were applied. Since group sizes in this study were completely equal (n = 5), for analysis, two-way ANOVAs of the histological data and repeated measures (RM) two-way ANOVAs of the MRE data were conducted, although not all data sets met the assumptions for an ANOVA. In the two-way ANOVA, Treatment represented the between-subjects factor and Time the within-subjects factor. In the RM two-way ANOVA, Time and Treatment by Time represented the within-subjects factors and Treatment the between-subjects factor. Pairwise comparisons applying the Bonferroni test were used to directly compare the two treatment groups within each time-point or the different time-points within each treatment group, respectively. All statistical analysis was conducted using SPSS Statistics 19 for Windows with the level of significance set at 0.05. The diagrams were prepared using GraphPad Prism 5.

Results

MPTP-induced Transient Increase of Brain Elasticity and Viscosity

We investigated how brain viscoelasticity is affected by a MPTP-induced dopamine deficit. MRE was performed one day before MPTP-treatment (to establish a baseline), and 3, 6, 10, 14 and 18 days after treatment cessation to determine viscoelastic changes as a consequence of dopamine depletion. The results of MRE measurements focussing on the hippocampus, the region that contains a highly neurogenic area (SGZ) modulated by dopamine, are shown in Figure 3 (a–d). No influence of time was seen in the control group for any of the MRE parameters. Mean values (± standard error of the mean, SEM) in the hippocampal region of controls were 4.608 (±0.719) kPa, 1.388 (±0.125) kPa, 4.816 (±0.705) kPa and 0.549 (±0.073) for G′, G″ abs(G*) and φ, respectively. Similar values were found in the entire brain of the control group with 5.234 (±0.564) kPa, 1.447 (±0.87) kPa, 5.432

($\pm$0.553) kPa and 0.574 ($\pm$0.034) for G′, G″ abs(G*) and φ, respectively. RM two-way ANOVA showed an overall effect of time on G′ ($F_{(5,40)} = 5.239$, p<0.001), G″ ($F_{(5,40)} = 9.669$, p<0.001) and abs(G*) ($F_{(5,40)} = 5.689$, p<0.001), a treatment by time effect on G′ ($F_{(5,40)} = 3.841$, p<0.01), G″ ($F_{(5,40)} = 4.240$, p<0.01) and abs(G*) ($F_{(5,40)} = 4.045$, p<0.01) in MPTP-treated mice, but no effect of treatment alone on G′ ($F_{(1,8)} = 3.758$, p = 0.089), G″ ($F_{(1,8)} = 1.378$, p = 0.274) and abs(G*) ($F_{(1,8)} = 3.979$, p = 0.081). Pairwise comparison between groups at different days using the Bonferroni test revealed a marked temporary MPTP-induced increase at 6 dpi of G′ (Figure 3a, p<0.01), G″ (Figure 3b, p<0.01) and abs (G*) (Figure 3c, p<0.01) towards 6971 (1019) kPa, 1767 (103) kPa, 7192 (1011) kPa in the hippocampus, which was still significant within the whole-brain region (Figure S1). Relative to baseline values, the changes of G′, G″ and abs(G*) at 6 dpi in the hippocampus were 51%, 27%, and 49% and 29%, 16%, and 28% in the whole brain, respectively. Since the phase angle φ (Figure 3d) remains unchanged by treatment ($F_{(1,8)} = 0.363$, p = 0.563) during the course of measurements ($F_{(5,40)} = 0.573$, p = 0.720), the findings suggest that the viscoelasticity of hippocampal tissue is selectively altered transiently after MPTP treatment without influencing the architecture of the cellular matrix.

MPTP-induced Transient Increase of New Neural Precursor Cells and Neurons

Figure 3 (e and f) shows cell numbers of new neurons (BrdU+/NeuN+) and precursor cells (BrdU+/+Nestin/GFP+) relative to the total number of BrdU-positive cells in the SGZ and GCL. Analysis by two-way ANOVA revealed a noticeable time effect on both cell types (BrdU+/Nestin/GFP+: $F_{(5,48)} = 9.070$, p<0.0001; BrdU+/NeuN+: $F_{(5,48)} = 41.910$, p<0.0001), but only a marginal interaction of both factors (BrdU+/Nestin/GFP+: $F_{(5,48)} = 2,146$, p = 0.076; BrdU+/NeuN+: $F_{(5,48)} = 2.095$, p = 0.082). Pairwise comparisons showed that mice treated with MPTP displayed a larger proportion of new precursor cells at 3 dpi (Figure 3e; p<0.05) and of new neurons at 6 dpi (Figure 3f; p<0.05) than controls regarding the total amount of newly generated cells. However, at 18 dpi, referring to the last day of MRE measurement, MPTP treatment appeared to provoke a reduced neurogenesis expressed as a smaller proportion of new neurons compared to controls (Figure 3f; p<0.05).

Absolute numbers of newly generated cells (BrdU+), new neural precursor cells and new neurons are shown in Figure 4 (b–d). Representative confocal images of BrdU and its colocalization with Nestin/GFP or NeuN, respectively, are shown in Figure 5. A two-way ANOVA revealed a strong influence of time on all three cell types (BrdU: $F_{(5,48)} = 19.336$, p<0.0001; BrdU/Nestin: $F_{(5,48)} = 12.542$, p<0.0001; BrdU/NeuN: $F_{(5,48)} = 13.920$, p<0.0001). Furthermore, the ANOVA also showed a treatment by time effect on newly generated precursor cells ($F_{(5,48)} = 2.768$, p<0.05). Pairwise comparison showed that in MPTP-treated mice, compared to controls, an increased proliferation of Nestin/GFP cells occurred until 3 dpi (Figure 4c; p<0.001) with a subsequent drop on 6 dpi (p<0.01, compared to MPTP at 3 dpi; not indicated in the figure) that may suggest a transient reactive proliferation of Nestin/GFP precursor cells in response to the neurotoxin as shown before in previous work from our group (27, 28). The observed course of BrdU-, new Nestin/GFP- und new NeuN-positive cell numbers over time generally parallels the suggested different stages during neuronal development including proliferation, survival and maturation [20].

MPTP-induced Increase of Microglia in the DG Region does not Change the Total Number of Cells in the GCL

The obtained numbers from stereological counting of DAPI-stained GCL/SGZ cells are shown in Figure 4a. Neither an overall effect of treatment ($F_{(1,48)} = 1.052$, p = 0.31) or time ($F_{(5,48)} = 0.382$, p = 0.859) alone nor an interaction between these factors ($F_{(5,48)} = 0.713$, p = 0.616) was found, indicating that the total number of GCL and SGZ cells was not affected by MPTP treatment and there was also no change in the total cell number over time.

Absolute numbers of all Iba1-positive cells in the GCL/SGZ, molecular layer and hilus are shown in Figure 4e. As a two-way ANOVA revealed, only time had an influence on the number of Iba1-positive cells ($F_{(5,48)} = 9.635$, p<0.0001). Pairwise comparisons showed that treatment groups differed at 3 dpi (p<0.05) with MPTP-treated mice displaying more microglia and macrophages in the DG region than their unaffected controls. However, numbers of Iba1-positive cells in mice treated with MPTP stay high, while controls then reach the same level of microglia and macrophages at 6 dpi.

Discussion

MPTP-induced degeneration of dopaminergic neurons affects neurogenesis in the hippocampus [24,28,29] and leads to changes in neural cell proliferation patterns in wide regions of the brain [24,25,27,39]. We observed for the first time that newly generated neurons in the DG potentially integrate with the mechanical scaffold of brain tissue yielding an apparent invigoration of the viscoelastic lattice with 50% increased shear modulus (G′) in MPTP-lesioned mice at 6 dpi. In comparison, the neuronal density in the SGZ/GCL changed only by 10% (see Figure 3f) thereby highlighting the sensitivity of macroscopic shear modulus to the number and type of cells engaged in the mechanical tissue matrix. This marked increase of shear elasticity as a result of reactively generated neurons induced by a dopamine deficit is in alignment with observations of [17] who demonstrated that, in contrast to our study, brain stiffness in a murine stroke model is reduced due to neuronal loss. Taken together both studies shed light onto the important role of neurons as a supporting structure of the brain's mechanical scaffold and complements recent results of in vivo MRE in volunteers and patients: A loss of neuronal support in the viscoelastic lattice of the brain may contribute to the disseminated decrease of G′ and G″ observed in the aging brain and in patients with NPH, AD and MS [10–14]. Given this pivotal role of neurons for the macroscopic mechanical properties of the brain, it is not surprising that cerebral MRE has been more sensitive to physiological aging than any other MRI method [13,40].

In general, the sensitivity of in vivo MRE arises from the scaling properties of mechanical constants. The shear modulus of a hierarchical system is determined by crosslinks in each existing level within the tissue's architecture towards microscopic interactions of cells [38]. Understanding the macroscopic mechanical response of our mouse model requires both knowledge about single-cell properties and how these properties would integrate into the multi-hierarchic lattice of the brain. Single neurons and glia cells taken from mouse brain tissue investigated by scanning force microscopy showed – similar to the bulk tissue – a higher storage modulus than loss modulus (G′>G″) with neurons being generally stiffer than glia cells [41]. This supports our proposed mechanistic explanation that the neuronal network establishes the primary mechanical backbone of the brain. In the bulk tissue, the ratio between elastic and viscose properties (as quantified by our loss tangent $\varphi = \arctan(G''/G')$) can give some insight into the
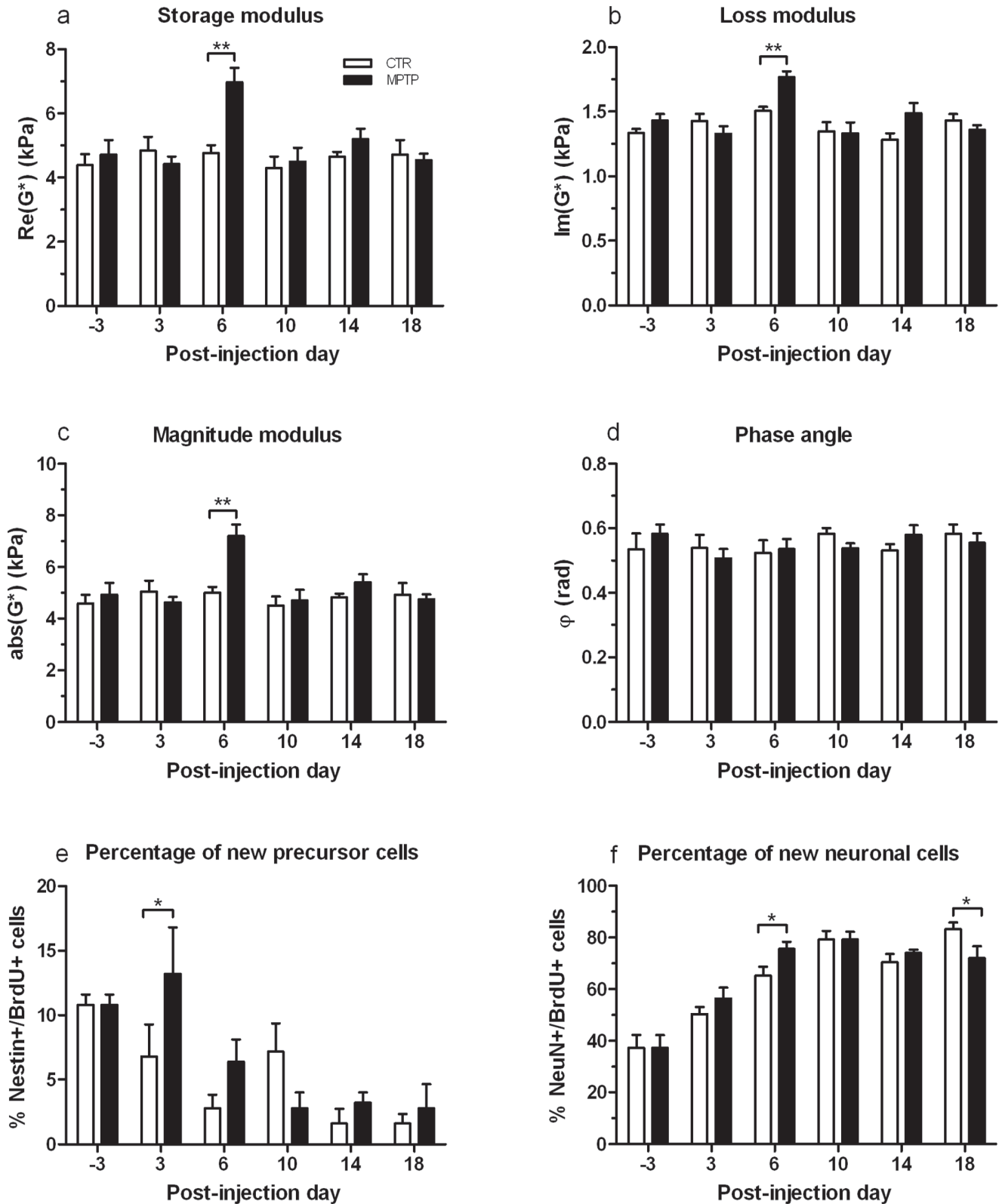
Figure 3. Variation of MRE parameters due to MPTP in the hippocampus of mice and results of cell counts in the DG. MPTP induced a transient increase of brain elasticity and viscosity (a, b and c) at 6 dpi, while the phase angle φ (d) remained unchanged (mean±SEM). Histologically, a transient MPTP-induced increase of new precursor cells (BrdU+/Nestin/GFP+) at 3 dpi (e) and of new neurons (BrdU+/NeuN+) at 6 dpi (f) as percentage of all newborn cells (BrdU+) was found (mean±SEM). *p<0.05, **p<0.01.
doi:10.1371/journal.pone.0092582.g003
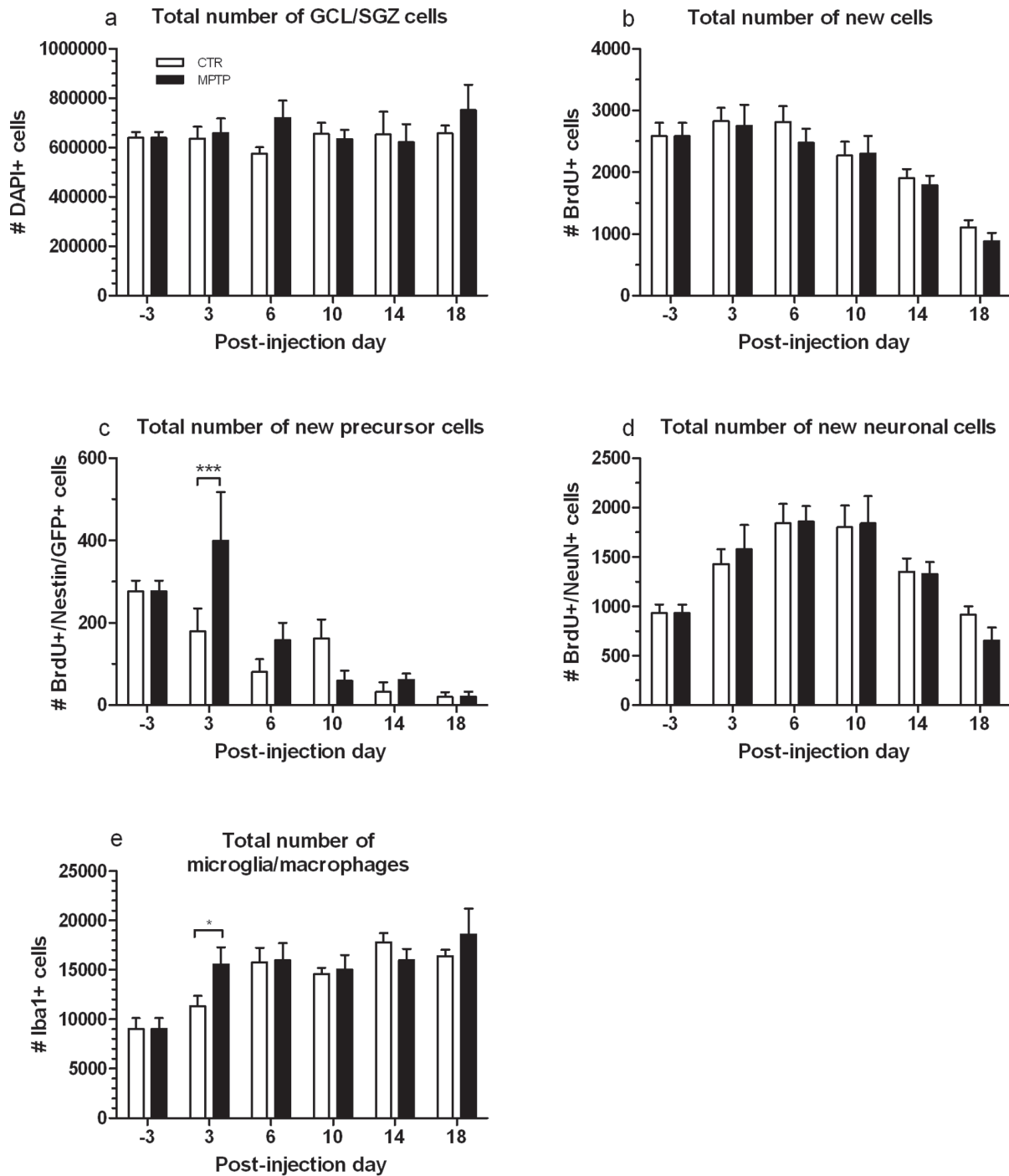
Figure 4. Results of cell counts in the DG. Fluorescence- and DAB-stained brain sections of MPTP-treated and CTR mice at the different time-points of MRE assessment, showing the total number of a) GCL/SGZ cells (DAPI), b) newborn cells (BrdU+), c) new precursor cells (BrdU+/Nestin/GFP+), d) new neuronal cells (BrdU+/NeuN+), and f) microglia and macrophages (Iba1+) in the GCL/SGZ, ML and hilus (mean±SEM). *p<0.05, **p<0.01.
doi:10.1371/journal.pone.0092582.g004

alteration of the geometrical arrangement of the mechanical networks. The nonsignificant alteration of φ in our data suggests that newly born neurons do not assemble a new network with own geometry at 6 dpi, shortly after their generation. They rather appear isolated yet as differentiation and maturation of newly generated cells into neurons and their functional integration into the present neuronal network by fully developing axons, dendrites

and synaptic links and thus being involved in the structure of the matured viscoelastic lattice takes about four weeks [20,42–45].

There is growing evidence that this process of adult neurogenesis is intimately connected with an intact neurotransmitter homeostasis, since dopamine depletion has been shown to cause disturbances in precursor cell proliferation [24,27–29]. Here, the analyses of newly generated cells in the DG, characterized as cells that incorporated the exogenous mitotic marker BrdU and its co-
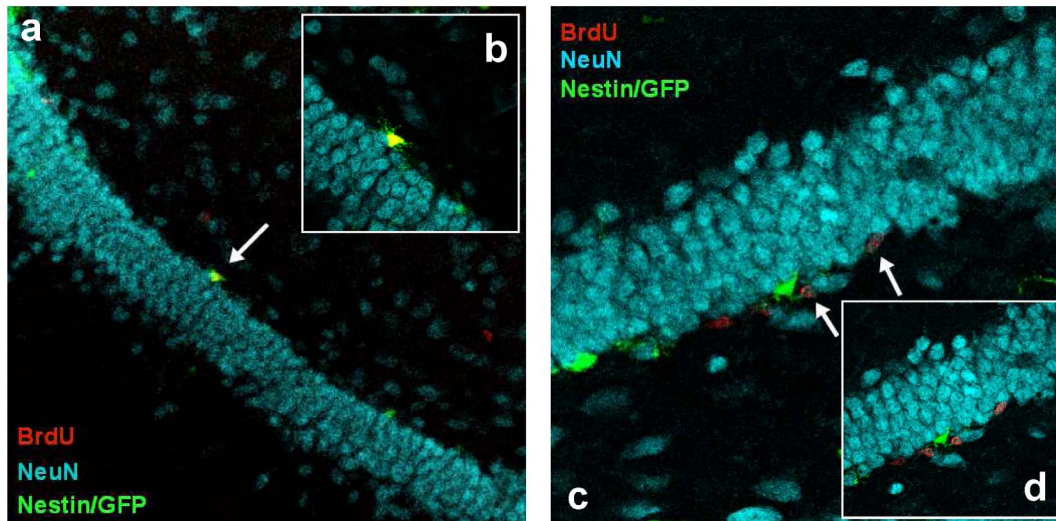
Figure 5. Representative confocal images of doublelabeled BrdU+/Nestin/GFP+ and BrdU+/NeuN+ cells. Mouse brain sections (40 μm) fluorescently stained with BrdU (red), NeuN (blue) and Nestin/GFP (green), showing the granular cell layer of the dentate gyrus with a Nestin/GFP-expressing precursor cell that is also positive for BrdU (a, 200×magnification and b, 630×magnification; arrow) and BrdU-positive cells coexpressing the neuronal marker NeuN (c, 400×magnification and d, 630×magnification; arrows).
doi:10.1371/journal.pone.0092582.g005

localization with Nestin/GFP to identify neural precursor cells, showed a marked transient increase of proliferated Nestin/GFP cells at 3 dpi in MPTP-lesioned mice. It is noteworthy that this rise occurred already at 3 dpi, while the transient gain in viscoelasticity was detected three days later at 6 dpi, which makes the proliferated neural precursor cells an unlikely candidate to account for the augmented stiffness. The observed increased number of proliferated precursor cells is in line with previous findings from our laboratory [27,28] demonstrating an acute and transient rise in new Nestin/GFP-positive cells in the DG and SNpc, respectively, shortly after MPTP treatment. We have previously shown a comparable stimulus-dependent selective regulation of different neural maturation stages in the DG [43,45]. The observed phenomenon possibly reflects a reactive neural precursor cell proliferation that may be, according to studies on other neurodegenerative processes, interpreted as an endogenous regenerative mechanism of the hippocampus to counteract neuronal injury in terms of keeping the endogenous stem-like cell pool at a stable level [46–49]. In the present study, the proportion of new neurons among all BrdU-positive cells at 6 dpi was higher in MPTP-lesioned mice than in unaffected animals. This finding suggests that the previous reactively generated precursor cells mature into neurons, which further supports the intended regenerative potential of the hippocampus. Unlike the Nestin/GFP-positive precursor cells, the increased neuron density three days later at 6 dpi, arisen from the enhanced precursor cell population in the DG, might have provoked the higher viscoelasticty values of the brain tissue at the same time-point. After this cellular gain up to 6 dpi, the proportion of new neurons slightly decreased until 18 dpi. From this, one could hypothesize that the pathological effect of MPTP is partially compensated by a transiently boosted proliferation of precursor cells without an increased net neurogenesis [29,39]. Additionally, although MPTP treatment modulated precursor cell proliferation and neurogenesis, it had no effect on the total amount of newborn BrdU-positive cells in the DG, which is in line with findings from other groups [29,39].

The neurotoxin MPTP is not only known to cause disturbances in neural cell proliferation and differentiation due to dopamine depletion but to also evoke an inflammatory reaction in affected brain areas including accumulation of microglia, lymphocytic infiltration and an increase in cytokine production [50], which might have been also a cause for the observed transient increase in brain elasticity. We addressed this issue by evaluating the number of microglia and macrophages in the DG area, which comprised the GCL/SGZ, molecular layer and hilus. We detected a peak in microglia and macrophages in MPTP-treated at 3 dpi, where no change in MRE measurements was observed. Although it appears unlikely that these inflammation-associated cell types contributed to the noticeable increase in brain viscoelasticity of MPTP-lesioned mice at 6 dpi, we can not preclude an inflammatory rise in extracellular fluid inducing an edematous swelling at a later time-point to be accountable for the observed brain stiffening. Due to the applied fixation method of the brain tissue for histological analysis, by which blood and other fluids are first washed out by PBS and then replaced by PFA, a potential edema is cleared out and not assessable anymore.

The synchrony of the transient MPTP-induced alteration of MRE parameters and neuronal cell density in our mouse model of dopamine depletion highlights the pivotal role of neurogenesis for brain elasticity. It is remarkable that Nestin/GFP-positive precursor cells do not alter MRE constants until their differentiation into NeuN-positive neurons. Hence, their mechanical properties must differ from those of neurons. It has already been demonstrated that neuronal cells are stiffer than glial cells [41], and that the elasticity of reactive glial cells depends on intermediate filament cell content [8]. In future experiments, neurons and neural precursor cells should be studied *in vitro*, applying MRE to analyse their individual mechanical properties and using histological and biomolecular techniques to correlate these mechanical characteristics with their cellular and molecular features. Interestingly, MRE seems to be more sensitive to the process of cell differentiation than histological cell counts and provides additional information about the dissemination of neuronal turnover. Albeit most enhanced in the hippocampus,

we observed a marked increase of G′, G″ and abs(G*) throughout the whole brain in a transverse image slice. This apparently diffuse pattern of transiently increased neurogenesis in the hippocampus due to MPTP treatment is a surprising result and motivates further investigations of the correlation between histology and viscoelastic parameters in different regions of the brain. With the current state of the art, MRE can provide consistent quantitative values on a global scale, i.e. considering spatially averaged constants. This permits the detection of diffuse pathology as has been demonstrated for NPH, AD and MS [11–14]. However, fast sampling methods and optimized reconstruction routines are being developed, which expand MRE towards a high resolution imaging modality [7,51,52].

When comparing human MRE with small animal studies, caution has to be taken: The higher dynamic range of MRE in the mouse (900 Hz in our study) compared to ∼50 Hz in humans may cause a shift in MRE sensitivity towards the loss properties of the tissue. Whether the complex shear modulus of brain tissue at low vibration frequencies would be sensitive to detecting the changes reported in this paper remains to be determined.

In the near future, viscoelastic constants of the brain may provide the missing link between morphometric imaging parameters and neuronal health on the cellular network level. Our results provide the first indication of the involvement of newly generated neurons into the viscoelastic matrix of the brain, corroborating the hypothesis that the neuronal network effectively contributes to the mechanical scaffold of the brain and therewith encourage further studies on humans for the clinical assessment of neural plasticity and neurodegeneration by MRE.

Supporting Information

Figure S1 Variation of MRE parameters due to MPTP in the whole brain. MPTP induced a transient increase of brain elasticity and viscosity (a, b and c) at 6 dpi, while the phase angle φ (d) remained unchanged (mean±SEM). *p<0.05, **p<0.01 (TIF)

Acknowledgments

Author Contributions

Conceived and designed the experiments: CK KR BS IS. Performed the experiments: CK EH KR SM. Analyzed the data: CK JB IS. Contributed reagents/materials/analysis tools: SM BS IS. Wrote the paper: CK BS IS.

References

1. Muthupillai R, Ehman RL (1996) Magnetic resonance elastography. Nat Med 2: 601–603.
2. Kruse SA, Rose GH, Glaser KJ, Manduca A, Felmlee JP et al. (2008) Magnetic resonance elastography in the brain. Neuroimage 39: 231–237.
3. Sack I, Beierbach B, Hamberger U, Klatt D, Braun J (2008) Non-invasive measurement of brain viscoelasticity using magnetic resonance elastography. NMR Biomed 21: 265–271.
4. Green MA, Bilston LE, Sinkus R (2008) In vivo brain viscoelastic properties measured by magnetic resonance elastography. NMR Biomed 21: 755–764.
5. Clayton EH, Genin GM, Bayly PV (2012) Transmission, attenuation and reflection of shear waves in the human brain. J R Soc Interface 9: 2899–2910.
6. Weaver JB, Pattinson AJ, McGarry MD, Perreard IM, Swienckowski JG et al. (2012) Brain mechanical property measurement using MRE in intrinsic activation. Phys Med Biol 57: 7275–7287.
7. Johnson CL, McGarry MD, Gharibans AA, Weaver JB, Paulsen KD et al. (2013) Local mechanical properties of white matter structure in the human brain. Neuroimage 79: 145–152.
8. Lu Y-B, Iandiev I, Hollborn M, Körber N, Ulbricht etal. (2011) Reactive glial cells: increased stiffness correlates with increased intermediate filament expression. FASEB J 25: 624–631.
9. Tully B, Ventikos Y (2011) Cerebral water transport using multiple-network poroelastic theory: application to normal pressure hydrocephalus. J Fluid Mech 667: 188–215.
10. Sack I, Streitberger KJ, Krefting D, Paul F, Braun J (2011) The influence of physiological aging and atrophy on brain viscoelastic properties in humans. PlosOne 6: e23451.
11. Streitberger K-J, Wiener E, Hoffmann J, Freimann FB, Klatt D et al. (2011) In vivo viscoelastic properties of the brain in normal pressure hydrocephalus. NMR Biomed 24: 385–392.
12. Murphy MC, Huston III J, Jack Jr CR, Glaser KJ, Manduca A et al. (2011) Decreased brain stiffness in Alzheimer's disease determined by magnetic resonance imaging. J Magn Reson Imaging 34: 494–498.
13. Streitberger K-J, Sack I, Krefting D, Pfueller C, Braun J et al. (2012) Brain viscoelasticity alteration in chronic-progressive multiple sclerosis. PlosOne 7: e29888.
14. Wuerfel J, Paul F, Beierbach B, Hamhaber U, Klatt D et al. (2010) MR-elastography reveals degradation of tissue integrity in multiple sclerosis. Neuroimage 49: 2520–2525.
15. Schregel K, Wuerfel née Tysiak E, Garteiser P, Gemeinhardt I, Prozorovski T et al. (2012) Demyelination reduces brain parenchymal stiffness quantified in vivo by magnetic resonance elastography. Proc Natl Aca Sci U S A 109: 6650–6655.
16. Riek K, Millward JM, Hamann I, Mueller S, Pfueller CF et al. (2012) Magnetic resonance elastography reveals altered brain viscoelasticity in experimental autoimmune encephalomyelitis. NeuroImage: Clinical 1: 81–90.
17. Freimann FB, Mueller S, Streitberger K-J, Guo J, Rot S et al. (2013) MR elastography in a murine stroke model reveals correlation of macroscopic viscoelastic properties of the brain with neuronal density. NMR Biomed 26: 1534–1539.
18. Lendahl U, Zimmermann LB, McKay RDG (1990) CNS stem cells express a new class of intermediate filament protein. Cell 60: 585–595.
19. Jessberger S, Kempermann G (2003) Adult-born hippocampal neurons mature into activity-dependent responsiveness. Eur J Neurosci 18: 2707–2712.
20. Kempermann G, Jessberger S, Steiner B, Kronenberg G (2004) Milestones of neuronal development in the adult hippocampus. Trends Neurosci 27: 447–452.
21. Van Praag H, Schinder AF, Christie BR, Toni N, Palmer TD et al. (2002) Functional neurogenesis in the adult hippocampus. Nature 415: 1030–1034.
22. Baker SA, Baker KA, Hagg T (2004) Dopaminergic nigrostriatal projections regulate neural precursor proliferation in the adult mouse subventricular zone. Eur J Neurosci 20: 575–579.
23. Borta A, Hoeglinger GU (2007) Dopamine and adult neurogenesis. J Neurochem 100: 587–595.
24. Höglinger GU, Rizk P, Muriel MP, Duyckaerts C, Oertel WH et al. (2004) Dopamine depletion impairs precursor cell proliferation in Parkinson disease. Nature Neurosci 7: 726–735.
25. Freundlieb N, Francois C, Tande D, Oertel WH, Hirsch EC et al. (2006) Dopaminergic substantia nigra neurons project topographically organized to the subventricular zone and stimulate precursor cell proliferation in aged animals. J Neurosci 26: 2321–2325.
26. Kippin TE, Kapur S, van der Kooy D (2005) Dopamine specifically inhibits forebrain neural stem cell proliferation, suggesting a novel effect of antipsychotic drugs. Neurobiol Dis 25: 5815–5823.
27. Klaissle P, Lesemann A, Huehnchen P, Hermann A, Storch A et al. (2012) Physical activity and environmental enrichment regulate the generation of neural precursors in the adult mouse substantia nigra in a dopamine-dependent manner. BMC Neurosci 13: 1–15.
28. Lesemann A, Reinel C, Huehnchen P, Pilhatsch M, Hellweg R et al. (2012) MPTP-induced hippocampal effects on serotonin, dopamine, neurotrophins, adult neurogenesis and depression-like behaviour are partially influenced by fluoxetine in adult mice. Brain Res 1457: 51–69.
29. Park J-H, Enikolopov G (2010) Transient elevation of adult hippocampal neurogenesis after dopamine depletion. Exp Neurol. 222: 267–276.
30. Yang P, Arnold SA, Habas A, Hetman M, Hagg T (2008) Ciliary neurotrophic factor mediates dopamine D$_2$ receptor-induced CNS neurogenesis in adult mice. J Neurosci 28: 2231–2241.
31. Gasbarri A, Sulli A, Packard MG (1997) The dopaminergic mesencephalic projections to the hippocampal formation in the rat. Prog Neuro-Psychopharmacol & Biol Psychiat 21: 1–22.
32. Gasbarri A, Verney C, Innocenzi R, Campana E, Pacitti C (1994) Mesolimbic dopaminergic neurons innervating the hippocampal formation in the rat: a combined retrograde tracing and immunohistochemical study. Brain Res 668: 71–79.
33. Kopin IJ (1987) MPTP: An industrial chemical and contaminant of illicit narcotics stimulates a new era in research on parkinson's disease. Environ. Health Perspect 75: 45–51.
34. Scatton B, Simon H, Le Moal M, Bischoff S (1980) Origin of dopaminergic innervation of the rat hippocampus. Neurosci Lett 18: 125–131.
35. Swanson LW (1982) The projections of the ventral tegmental area and adjacent regions: a combined fluorescent retrograde tracer and immunofluorescence study in the rat. Brain Res Bull 9: 321–353.

36. Clayton EH, Garbow JR, Bayly PV (2011) Frequency-dependent viscoelastic parameters of mouse brain tissue estimated by MR elastography. Phys Med Biol 56: 2391–2406.

37. Papazoglou S, Hamhaber U, Braun J, Sack I (2008) Algebraic Helmholtz inversion in planar magnetic resonance elastography. Phys Med Biol 53: 3147–3158.

38. Posnansky O, Guo J, Hirsch S, Papazoglou S, Braun J et al. (2012) Fractal network dimension and viscoelastic powerlaw behavior: A modeling approach based on a coarse-graining procedure combined with shear oscillatory rheometry. Phys Med Biol 57: 4023–4040.

39. Peng J, Xie L, Jin K, Greenberg DA, Andersen JK (2008) Fibroblast growth factor 2 enhances striatal and nigral neurogenesis in the acute 1-methyl-4-phenyl-1,2,3,6-tetrahydropyridine model of parkinson's disease. Neuroscience 153: 664–670.

40. Sack I, Beierbach B, Wuerfel J, Klatt D, Hamhaber U et al. (2009) The impact of aging and gender on brain viscoelasticity. Neuroimage 46: 652–657.

41. Lu Y-B, Franze K, Seifert G, Steinhaeuser C, Kirchhoff F et al. (2006) Viscoelastic properties of individual glial cells and neurons in the CNS. Proc Natl Acad Sci U S A 103: 17759–17764.

42. Kronenberg G, Reuter K, Steiner B, Brandt MD, Jessberger S et al. (2003) Subpopulations of proliferating cells of the adult hippocampus respond differently to physiologic neurogenic stimuli. J Comp Neurol 467, 455–463.

43. Steiner B, Kronenberg G, Jessberger S, Brandt MD, Reuter K et al. (2004) Differential regulation of gliogenesis in the context of adult hippocampal neurogenesis in mice. Glia 46: 41–52.

44. Steiner B, Klempin F, Wang L, Kott M, Kettenmann H et al. (2006) Type-2 cells as link between glial and neuronal lineage in adult hippocampal neurogenesis. Glia 54: 805–814.

45. Steiner B, Zurborg S, Hoerster H, Fabel K, Kempermann G (2008) Differential 24 h responsiveness of Prox1-expressing precursor cells in adult hippocampal neurogenesis to physical activity, environmental enrichment, and kainic acid-induced seizures. Neuroscience 154: 521–529.

46. Aharoni R, Arnon R, Eilam R (2005) Neurogenesis and neuroprotection induced by peripheral immunomodulatory treatment of experimental autoimmune encephalomyelitis. J Neurosci 25: 8217–8228.

47. Arvidsson A, Collin T, Kirik D, Kokaia Z, Lindvall O (2002) Neuronal replacement from endogenous precursors in the adult brain after stroke. Nat Med 8: 963–970.

48. Gage FH, Kempermann G, Palmer TD, Peterson DA, Ray J (1998) Multipotent progenitor cells in the adult dentate gyrus. J Neurobiol 36: 249–266.

49. Huehnchen P, Prozorovski T, Klaissle P, Lesemann A, Ingwersen J et al. (2011) Modulation of adult hippocampal neurogenesis during myelin-directed autoimmune neuroinflammation. Glia 50: 132–142.

50. Kurkowska-Jastrzebeska I, Wronska A, Kohutnicka M, Czlonkowski A, Czlonkowska A (1999) The inflammatory reaction following 1-methyl-4-phenyl-1,2,3,6-tetrahydropyridine intoxication in mouse. Exp Neurol 156: 50–61.

51. Barnhill E, Kennedy P, Hammer S, van Beek EJ, Brown C et al. (2013) Statistical mapping of the effects of knee extension on thigh muscle viscoelastic properties using magnetic resonance elastography. Physiol Meas 34: 1675–1698.

52. Guo J, Hirsch S, Fehlner A, Papazoglou S, Scheel M et al. (2013) Towards an elastographic atlas of brain anatomy. PlosOne 8: e71807.

SCIENTIFIC REP⚙RTS

Only watching others making their experiences is insufficient to enhance adult neurogenesis and water maze performance in mice

Deetje Iggena[1], Charlotte Klein[1], Alexander Garthe[2,3], York Winter[4], Gerd Kempermann[2,3] & Barbara Steiner[1]

In the context of television consumption and its opportunity costs the question arises how far experiencing mere representations of the outer world would have the same neural and cognitive consequences than actively interacting with that environment. Here we demonstrate that physical interaction and direct exposition are essential for the beneficial effects of environmental enrichment. In our experiment, the mice living in a simple standard cage placed in the centre of a large enriched environment only indirectly experiencing the stimulus-rich surroundings (IND) did not display increased adult hippocampal neurogenesis. In contrast, the mice living in and directly experiencing the surrounding enriched environment (DIR) and mice living in a similar enriched cage containing an uninhabited inner cage (ENR) showed enhanced neurogenesis compared to mice in control conditions (CTR). Similarly, the beneficial effects of environmental enrichment on learning performance in the Morris Water maze depended on the direct interaction of the individual with the enrichment. In contrast, indirectly experiencing a stimulus-rich environment failed to improve memory functions indicating that direct interaction and activity within the stimulus-rich environment are necessary to induce structural and functional changes in the hippocampus.

The exposure to environmental enrichment is beneficial for structural and functional changes in the brain. Living in an enriched environment enhances the survival of newborn neurons in the hippocampus of adult mice, whereas physical activity predominantly stimulates the proliferation of hippocampal precursor cells[1,2]. Both external stimuli are additive and thus lead to a remarkable net increase in adult neurogenesis[3]. In several studies, this increased amount of newborn neurons has been linked to the improvement of certain hippocampal-dependent functions including spatial learning[1,3–6]. These observations relate to the medical observation that physical and cognitive activity reduce the risk of memory decline and neurodegenerative disorders[7,8].

As "activity" promotes neurogenesis, motility in a stimulus-rich world might be a strong modulator of neurogenesis-related function. Indeed, in a longitudinal study individual levels of active exploration and territorial coverage ("roaming entropy") correlated with adult hippocampal neurogenesis[9]. However, an enriched environment is more than merely an incentive for increased levels of motility. Instead it represents a complex inanimate and social stimulation consisting of multiple factors in numerous domains[10].

[1]Department of Neurology, Charité Universitätsmedizin, Charitéplatz 1, 10117 Berlin. [2]German Center for Neurodegenerative Diseases (DZNE) Dresden, Arnoldstraße 18, 01307 Dresden. [3]CRTD – Center for Regenerative Therapies Dresden, Technische Universität Dresden, Fetscherstraße 105, 01307 Dresden. [4]Institute of Biology and Berlin Mouse Clinic for Neurology and Psychiatry, Humboldt-Universität Berlin, Dorotheenstraße 96, 10117 Berlin. Correspondence and requests for materials should be addressed to G.K. (email: gerd.kempermann@dzne.de) or B.S. (email: barbara.steiner@charite.de)
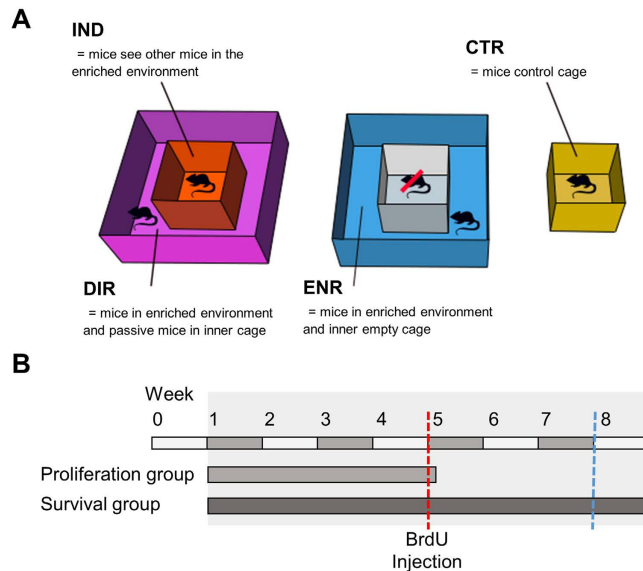
Figure 1. Experimental set-up. (**A**) Housing conditions. Mice lived in and directly experienced an enriched environment (DIR) while the mice in the inner standard cage indirectly experienced the surrounding enriched environment and its inhabitants (IND). Mice lived in an enriched environment which contained an uninhabited inner cage (ENR). Mice lived in a standard cage without any confrontation to environmental enrichment (CTR). The measures of the ENR/DIR cage: 0.74 m × 0.3 m × 0.74 m (W/H/D), the measures of the CTR/IND cage: 0.27 m × 0.15 m × 0.42 m (W/H/D). (**B**) Experimental timeline. Mice received three BrdU-injections on day 28 of the experiment. To assess cell proliferation mice were killed 24h after injection, to investigate cell survival mice were killed four weeks after injection. Spatial memory was assessed during the eighth week of the experiment.

Due to the complexity of an enriched environment the extent to which individual identifiable factors, including cognitive stimuli, contribute to the positive overall outcome has remained largely unknown.

Usually, mice living in an enriched environment are able to directly interact with their stimulating surrounding[1,3,6,10]. However, considering that a sedentary lifestyle is increasingly common we were in particular interested in the effects of indirect exposure and passive confrontation with such an environment[11]. We asked whether active participation is required for the beneficial effects of environmental enrichment on the brain or whether the merely indirect exposure to sights, sounds and odors of other mice directly experiencing that environment would be sufficient to enhance adult hippocampal neurogenesis. To answer this question we randomly assigned our mice to four different housing conditions (Fig. 1A) and exposed them either directly or indirectly to environmental enrichment for four or eight weeks (Fig. 1B). We conducted histological studies to investigate adult hippocampal neurogenesis and tested the mice in the Morris water maze to assess spatial memory as example of potential functional consequences.

Results

Direct interaction with environmental enrichment increases the survival of newborn neurons. Adult neurogenesis was assessed by the standard methodology based on bromodeoxyuridine (BrdU)-incorporation into the dividing precursor cells and immunohistochemical analysis of their progeny[12]. Typically for the enrichment paradigm, direct exposure to the environmental enrichment elicited a strong pro-survival effect on newborn cells four weeks after BrdU-incorporation (Fig. 2A,B; $F_{3,25} = 13.809$, $P < 0.001$; post-hoc: ENR versus CTR, $P < 0.001$; DIR versus CTR, $P = 0.001$). However, this beneficial effect on neurogenesis was absent in the IND group with prohibited direct interaction and only indirect exposure to an enriched environment (IND versus CTR, $P = 0.227$). We further explored whether the observed difference was due to an increased number of newborn neurons by estimating BrdU$^+$/NeuN$^+$ colabeling. ENR and DIR showed significantly more NeuN-positive neurons than CTR (Fig. 2C; $F_{3,25} = 11.673$, $P < 0.0001$; post-hoc: ENR versus CTR, $P < 0.001$; DIR versus CTR; $P = 0.003$) while the indirect exposure did not affect neuronal differentiation (IND versus CTR, $P = 0.401$) suggesting that indirect exposure is an inadequate stimulus for adult neurogenesis. Instead, direct interaction is required to enhance the survival of newborn neurons.

Hippocampal cell proliferation remains unaffected by environmental enrichment. We next examined hippocampal proliferation in transgenic Nestin-GFP mice using BrdU-immunohistochemistry and determined the different subpopulations of neuronal precursor cells by colabeling for neuronal
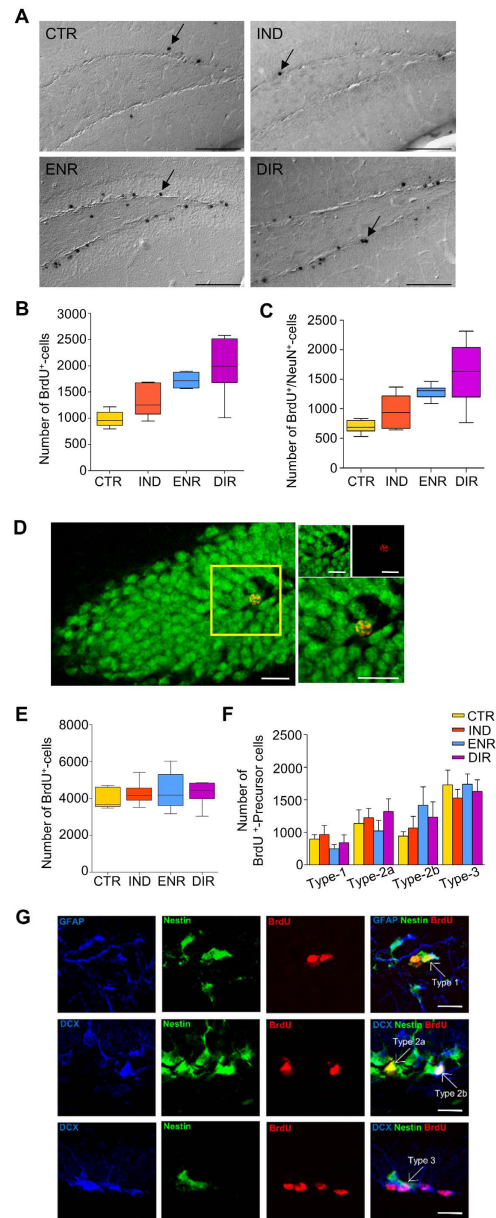
Figure 2. Newborn cells in the granule cell layer of the dentate gyrus. (**A**) Representative DIC-images of BrdU-immunohistochemistry in CTR, IND, ENR and DIR showing four weeks old cells. Arrows highlight exemplary BrdU$^+$-cells. Scale bar, 100 μm. (**B**) Absolute number of survived BrdU$^+$-cells four weeks after BrdU-incorporation. ENR and DIR displayed significantly more cells (ENR versus CTR, P < 0.001; DIR versus CTR, P = 0.001) while IND and CTR did not differ (IND versus CTR, P 0.227). (**C**) Absolute number of survived neurons colabeled by BrdU and the neuronal marker NeuN. ENR and DIR (ENR versus DIR, P = 0.481) did not differ, but showed increased neurogenesis compared to CTR (ENR versus CTR, P < 0.001; DIR versus CTR, P = 0.003) while IND did not differ from CTR and ENR (IND versus CTR, P = 0.401; IND versus ENR, P = 0.219), but from DIR (IND versus DIR, P = 0.048). CTR, N = 7; IND, N = 6; ENR, N = 7; DIR, N = 9. (**D**) Representative confocal images of NeuN$^+$ (green)/BrdU$^+$ (red) cells appearing orange when colabeled. Scale bars 20 μm. (**E**) Absolute number of BrdU$^+$-cells 24 hours after BrdU-incorporation. Environmental enrichment did not affect cell proliferation rate (P = 0.761). CTR, N = 5; IND, N = 6; ENR, N = 5; DIR, N = 10. (**F**) Absolute number of BrdU$^+$-cells in the subpopulations of hippocampal proliferating neurons 24 hours after BrdU-incorporation. Environmental enrichment did not affect any neuronal subpopulation of precursor cells. (**G**) Representative confocal images of BrdU-colabeled type 1 (GFAP$^+$/Nestin$^+$), type 2a (Nestin$^+$), type 2b (Nestin$^+$/Dcx$^+$) and type 3 (Dcx$^+$) neuronal precursor cells. Scale bars 20 μm. Data presented as boxplots with a centre line as median, Tukey-style whiskers extend 1.5 times the interquartile range from 25th and 75th percentiles and dots represent outliers. Numbers of precursor cells shown as mean± s.e.m.

markers[13,14]. As predicted, neither direct nor indirect exposure to an enriched environment increased hippocampal cell proliferation 24 hours after BrdU-incorporation (Fig. 2E; $F_{3,22} = 0.391$; $P = 0.761$). Similarly, our additional investigations revealed no differences in the subtypes of neuronal precursor cells (Fig. 2F). The groups neither differed in the number of type 1, Nestin$^+$/GFAP$^+$-cells, ($F_{3,17} = 0.730$, $P = 0.548$) type 2a, Nestin$^+$-cells, ($F_{3,21} = 0.467$, $P = 0.709$) type 2b, Nestin$^+$/Dcx$^+$-cells ($F_{3,21} = 0.704$, $P = 0.560$) nor type 3, Dcx$^+$-cells, ($F_{3,21} = 0.271$, $P = 0.846$) cells. The histological analysis indicates that the beneficial effects of direct interaction with an enriched environment are in particular due to survival-promoting effects instead of increasing the cell proliferation rate or influencing the distribution of the different subpopulations of neuronal precursor cells.

Direct interaction with environmental enrichment improves Morris water maze performance. We next related our morphological results to behavioral data. Our mice were tested in a modified reversal learning version of the Morris water maze task that is able to detect alterations in cognitive performance associated with adult neurogenesis[15]. All groups started from the same base line showing no differences regarding the length of swim path during the first trial of day 1 ($F_{3,37} = 0.603$, $P = 0.617$) and performed similar over the entire first day. As indicated by the number of crossings at the previous goal location during the first trial after moving the platform to another quadrant all groups learned the task well (Fig. 3A; $F_{3,37} = 0.216$, $P = 0.885$). Additionally, no differences were found for swim path lengths during the first trial following goal reversal (day 4, $F_{3,37} = 0.599$, $P = 0.620$).

Environmental enrichment had the anticipated beneficial effect on task performance compared to CTR. Post-hoc analysis over all trials revealed that the average swim path to the hidden platform was significantly shorter in ENR (Fig. 3B; Repeated measures ANOVA: $F_{3,241} = 10.343$, $P < 0.001$; post-hoc: ENR versus CTR, $P = 0.030$). This effect appeared to be particular strong at the end of the acquisition phase (day 3, $F_{3,242} = 6.920$, $P < 0.001$; post-hoc: ENR versus CTR, $P = 0.031$). Interestingly, although DIR experienced the same length of exposure to environmental enrichment as mice from the ENR group, the swim path to target shown by DIR mice did not differ from CTR (over all days: DIR versus CTR, $P = 0.999$) nor on any single day (Day 1: $P = 0.135$; day 2: $P = 0.154$; day 3: $P = 0.961$; day 4: $P = 0.971$; day 5: $P = 1.000$). On the second day, DIR even appeared to perform worse than ENR ($F_{3,242} = 6.248$, $P < 0.001$ post-hoc: ENR versus DIR, $P = 0.050$).

Even more surprising was the observation that IND performed worse than CTR in the water maze. Over all trials, IND showed significantly longer swim paths to target (IND versus CTR, $P = 0.036$). This discrepancy became particularly apparent on day 2 (IND versus CTR, $P = 0.012$), while on day 4 at least a trend to difference was observable ($F_{3,242} = 5.078$, $P = 0.002$; IND versus CTR, $P = 0.076$). These results suggest that the merely indirect exposure to environmental enrichment is insufficient to improve spatial memory and might even induce certain adverse effects on memory formation.

In addition to this overall analysis of water maze performance, we assessed the effect of different types of enrichment on distinct learning phases. We analyzed the swim path to target separately during acquisition (days 1 to 3) and reversal (days 4 and 5). Remarkably, the inferiority of IND compared to CTR was predominantly present during the reversal phase. While the analysis revealed a difference between IND and CTR on days 4 and 5 (Repeated measures ANOVA: $F_{3,242} = 7.549$, $P < 0.0001$; post-hoc: IND versus CTR, $P = 0.032$), no difference between IND and CTR during acquisition could be detected (Repeated measures ANOVA: $F_{3,241} = 6.397$, $P < 0.001$; post-hoc: IND versus CTR, $P = 0.379$). These results indicate that in IND memory is especially affected in terms of flexibility and the ability to relearn. A similar pattern was revealed comparing DIR to ENR: during acquisition DIR and ENR performed similarly ($P = 0.730$), but reversal analysis revealed a trend to worse performance in DIR mice, which however remained statistically insignificant ($P = 0.087$). Neither during acquisition nor during reversal DIR differed from CTR ($P = 0.881$ and $P = 0.987$, respectively). The "normal" enrichment group ENR displayed a trend to differ from CTR during acquisition ($P = 0.084$), while there was no evidence of a difference between ENR and CTR during reversal ($P = 0.349$). It seems that while ENR possibly outperformed CTR during acquisition, IND and DIR were unable to do likewise and even performed worse during reversal compared to CTR and ENR, respectively. Flexibility seems to be the main aspect of memory formation to be affected by the experimental design of indirect versus direct exposure to environmental enrichment, thereby contributing to the reduced overall performance of IND and DIR in the Morris water maze (Fig. 4).

Direct interaction with environmental enrichment enhances the quality of spatial learning. We next analyzed qualitative aspects of the spatial learning. First, we plotted the presence probability of the mice in the circular water maze arena. On day 4, the heatmap visualizes the faster reversal learning in ENR. ENR evolved a clear local preference for the new target already during the third trial, whereas the other groups struggled to develop a new preference. Even in DIR a new strong local preference for the new platform location did not evolve as quickly as in ENR. This fits the observation that DIR required a longer swim path to the target than ENR. However, group differences regarding the average distance to target could not be revealed, but between IND and ENR during the third trial on day 4 (($F_{3,37} = 4.786$, $P = 0.006$, IND versus ENR, $P = 0.004$). Second, we investigated the efficiency of the chosen search strategies and whether these strategies were hippocampus-dependent. To classify the search strategies the sequence of xy-coordinates was analysed using an algorithm introduced previously[15]. The
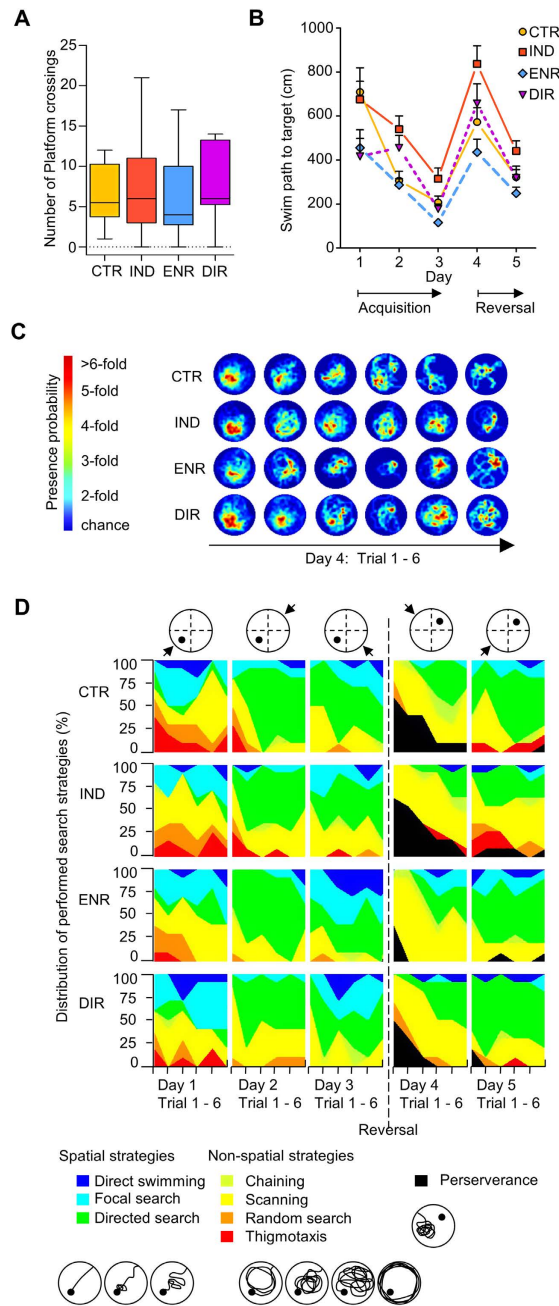
Figure 3. Performance in a reversal-learning type of the Morris water maze. (**A**) All groups learned to navigate to the platform during the acquisition phase (days 1 to 3) thus the groups did not differ in the total number of crossing of the previous target zone during the first trial on day four after the platform was relocated. (P = 0.885). (**B**) The ability to reach the platform as fast as possible differed between the groups. ENR displayed a significantly shorter swim path than CTR while DIR only differed from IND but not from CTR. IND needed even a significantly longer swim path than CTR. (IND versus ENR, P < 0.001; IND versus DIR, P = 0.016; CTR versus ENR, P = 0.030; CTR versus IND, P = 0.036; ENR versus DIR, P = 0.141; CTR versus DIR, P = 0.999) (**C**) Heatmaps depict the development of spatial preferences in the water tank after the platform had been relocated into the opposite quadrant on day four. Although no statistical difference regarding distance to target could be revealed but between IND and ENR in trial 3 ($F_{3,37}$ = 4.786, P = 0.006, IND versus ENR, P = 0.004), the heatmaps visualize ENR's faster reversal learning and development of a local preference for the new target already during the third trial while the other groups struggled to develop a new preference. (**D**) Distribution of performed search-strategies during the five days. IND used more inefficient non-spatial strategies to reach the goal than expected (Chi-square = 34.276, P < 0.001; IND 58.4%, CTR 43.9%, DIR 42.1%, ENR 35.4%). Number of platform crossings presented as boxplots with a centre line as median, Tukey-style whiskers extend 1.5 times the interquartile range from 25th and 75th percentiles. Swim path to target presented as mean± s.e.m. CTR, N = 10; IND, N = 11; ENR, N = 10; DIR, N = 10.

	CTR	IND	ENR	DIR
Survival of newborn cells (BrdU$^+$-cells)	986.57 ± 54.49	1323.50 ± 123.78 (P = 0.227) ➡	1710.00 ± 52.31 (P < 0.001) ⬆	2014.00 ± 170.98 (P = 0.001) ⬆
Survival of newborn neurons (BrdU$^+$/NeuN$^+$-cells)	689.36 ± 39.57	955.67 ± 121.60 (P = 0.401) ➡	1288.19 ± 44.37 (P < 0.001) ⬆	1602.26 ± 167.89 (P = 0.003) ⬆
Proliferation of newborn precursor cells (BrdU$^+$-cells)	4010.40 ± 250.77	4259.00 ± 256.15 ➡	4400.40 ± 464.69 ➡	4479.00 ± 283.20 ➡
Number of type 1 cells (GFAP$^+$/Nestin$^+$ -cells)	395.78 ± 68.80	466.44 ± 137.80 ➡	248.33 ± 63.74 ➡	339.62 ± 120.66 ➡
Type 2a cells (Nestin$^+$-cells)	635.85 ± 209.09	723.20 ± 140.24 ➡	521.13 ± 163.32 ➡	819.49 ± 193.12 ➡
Type 2b cells (Nestin$^+$/Dcx$^+$-cells)	440.28 ± 71.26	566.98 ± 180.55 ➡	916.82 ± 282.88 ➡	734.08 ± 234.75 ➡
Type 3 cells (Dcx$^+$-cells)	1229.62 ± 223.73	1024.46 ± 135.07 ➡	1238.46 ± 156.95 ➡	1126.60 ± 180.46 ➡
Length of swim path (day 1 – 5)	423.56 ± 42.56cm	547.60 ± 29.44cm ⬆ (P = 0.036)	308.48 ± 22.96cm ⬇ (P = 0.030)	405.36 ± 30.48cm P = 0.999 ➡
Length of swim path (day 1)	709.23 ± 98.55cm	675.53 ± 82.65cm (P = 1.000) ➡	455.82 ± 81.46cm (P = 0.264) ➡	416.58 ± 81.45cm (P = 0.135) ➡
Length of swim path (day 2)	306.22 ± 42.67cm	540.29 ± 60.18cm ⬆ (P = 0.012)	286.64 ± 28.53cm (P = 0.999) ➡	455.88 ± 55.98cm (P = 0.154) ➡
Length of swim path (day 3)	207.29 ± 29.0 cm	315.03 ± 48.29cm (P = 0.303) ➡	116.0 ± 13.07cm (P = 0.031) ⬇	177.49 ± 22.52cm (P = 0.961) ➡
Length of swim path (day 4)	572.60 ± 65.59cm	837.29 ± 82.02cm (P = 0.076) ➡	435.40 ± 59.95cm (P = 0.552) ➡	657.29 ± 89.22cm (P = 0.971) ➡
Length of swim path (day 5)	322.45 ± 49.75cm	440.82 ± 46.89cm (P = 0.417) ➡	248.53 ± 28.39cm (P = 0.738) ➡	319.58 ± 37.37cm (P = 1.000) ➡
Length of swim path (acquisition, day 1 – 3)	407.58 ± 40.28cm	502.02 ± 38.10cm (P = 0.379) ➡	286.15 ± 30.74cm (P = 0.349) ➡	349.98 ± 34.83cm (P = 0.881) ➡
Length of swim path (reversal, day 4 – 5)	447.52 ± 26.92cm	615.60 ± 48.19cm ⬆ (P = 0.032)	341.96 ± 34.12cm (P = 0.084) ➡	488.43 ± 50.59cm (P = 0.987) ➡
Non-spatial search strategies (day 1 – 5)	43.9% [a]	53.8% [b] (P < 0.001) ⬆	42.1% [a] ➡	35.4% [a] ➡
Choice of perseverance as strategy (day 4)	28.3% [a]	31.3% [a] ➡	6.7% [b] (P = 0.002) ⬇	15.3% [ab] ➡

Figure 4. Table of results. Showing an overview of the experimental results regarding histology, length of swim path and choice of search strategies during the Morris water maze. The groups IND, ENR and DIR are compared to CTR. Data is presented as mean value ± s.e.m. In case of significant main effects, the p-value of the followed post-hoc analysis is presented.

statistical analysis of independence revealed that IND mice more often used hippocampus independent non-spatial like thigmotaxis, random search, scanning and chaining and thus chose less efficient strategies to navigate to the platform than compared to control and the other groups would have been expected (Fig. 3D; chi-square (3) = 34.276, P < 0.001, IND (53.8%) versus CTR (43.9%), DIR (42.1%), ENR (35.4%)). This result adds qualitative details to the observed prolonged latency and swim paths to the platform and indicates that functional plasticity is reduced in IND compared to CTR. With respect to "perseverance", characterized by an incorrect, prolonged preference for the previous goal on day 4, ENR persevered less than CTR and IND (chi-square (21) = 44.782, P = 0.002, IND (31.3%), CTR (28.3%), DIR (15.3%), ENR (6.7%)). This is matching the impression that can be gained from the heatmaps. The general preference of other strategies than perseverance probably contributes to the overall superior performance of ENR (Fig. 4).

Discussion

Our data indicate that the beneficial effects of environmental enrichment depend on the direct interaction of the individual with that environment. In contrast, merely watching (as well as hearing and smelling) other mice directly experiencing that stimulus-rich environment was insufficient to enhance adult hippocampal neurogenesis and failed to improve memory functions. The prevented direct interaction of the mice with environmental enrichment and other mice close-by even seems to have certain adverse effects on spatial learning.

Generally, our study confirms that environmental enrichment is a strong extrinsic neurogenic stimulus. But we also found the three groups experiencing enrichment in the present experiment (DIR,

IND and ENR) to be benefitting differently from the external stimulation. It appeared, for example, that the beneficial effects of an enriched environment on spatial memory were less pronounced in the DIR group than in the classical ENR group. These data were surprising at first. Potential confounders have to be discussed, which would result in a reduced enhancement of spatial memory by environmental enrichment that otherwise is known to be a robust stimulus of learning and memory performance and adult neurogenesis. However, both DIR and ENR groups had indeed the exact same floor size and cage design with the same possibility for physical activity and inter-individual stimulation, but ENR lacked mice in the inner cage. Possibly, the mice living in the inner cage acted as a distracting factor for DIR and thus reduced the positive impact of environmental enrichment on water maze performance. This might likewise apply to IND, which showed the poorest performance in the Morris water maze task. Also here the cage size and design were exactly the same as in CTR. The surroundings of the cages and the experimenters and animal care takers did not change over the experiment period to avoid the potential influence of an additional stimulation or stress. It might be that the proximity of other mice, which are only separated from the own group by a transparent wall, influenced hippocampus-dependent cognitive functions. Potentially, this effect was provoked by the inability of the two groups to directly interact with each other. This observation raises interesting questions about the role of social interactions in the effects elicited by environmental enrichment[16].

A study from the 1970s is in line with our findings, reporting that rats observing other rats in environmental enrichment neither displayed increased brain weight nor improved exploratory behavior[17]. Similarly, passive motion in a visually stimulating environment did not enhance performance in visual-spatial discrimination tasks[18]. Neither adult hippocampal neurogenesis nor spatial memory have been investigated in these paradigms.

Another study has confronted mice with a locked running-wheel, which, surprisingly, resulted in an increase in cell proliferation in the hippocampus[19]. Even though in that study the running-wheel could not be used for running, the mice could still directly interact with the running-wheel which thus by itself might be sufficient to contribute to enrichment, resulting in the observed effect on adult neurogenesis. We did not see a similar effect on hippocampal cell proliferation in any of our groups though, which is consistent with the prevailing notion that enriched environments primarily affect cell survival rather than precursor cell proliferation.

That previous evidence is also relevant with respect to the obvious notion that the levels of physical activity will have differed between our groups. Given that as yet no monitoring system is available that would allow measuring the low levels of motility in our cage-in-cage set up we do not know to what exact degree our groups differed in this respect. However, in none of the groups in the larger enriched cages did we observe increased precursor cell proliferation as it is normally displayed by mice with access to a running wheel[2]. In fact, it was the expected survival-promoting effect on newborn neurons that resulted in increased levels of adult neurogenesis in ENR and DIR.

Physical inactivity and the mere indirect exposure to external stimulation are characteristic of a sedentary lifestyle as it is found in modern humans. Such sedentary lifestyle is characterized by sitting in conjunction with excessive television consumption and computer use and is associated with increased morbidity and mortality[20-23]. Even though a direct transfer of our results to a human lifestyle is not advisable, cautious extrapolation to the human condition can be instructive since inactivity strongly interferes with mental and physical health[20-23].

While the "couch-potato analogy" is tempting and suggestive, a cautionary note is nevertheless required: we have been studying a highly reductionistic situation in mice. Lifestyle is a far more complex event consisting of multiple contributing factors. However, investigations in inbred mice with constant genetic factors enable scientists to assess the exclusive impact of emblematic environmental constellations in laboratory animals thus providing the opportunity to deepen our understanding of extrinsic neurogenic stimulation.

At present, few good experimental models are available to elucidate the complexity of lifestyle compounds and lifestyle interventions[24]. Some researcher consider housing in a standard cage as model for inactivity, while other researchers have introduced an audio-visual overstimulation paradigm for infant mice resembling a television-like set-up and revealed ensuing deficits in cognitive performance[25,26].

Despite all limitations and potential confounders, our findings are first experimental steps in addressing the biological basis of the more extensive multifactorial situation in humans. In the future, advanced lifestyle experiments are needed to assess the consequences of unhealthy lifestyles. In any case, our results do support the clear indications that physical activity and direct interaction with the environment is superior to second-hand experience.

Materials and Methods

Animals. A total number of 97 female mice at the age of six to seven weeks were assigned to our experiment. 71 C57Bl/6N mice were purchased from Charles River for the assessment of cell survival and spatial memory while 26 transgenic Nestin-GFP mice, expressing green fluorescent protein under the promotor of nestin on a C57Bl/6N background, were obtained from FEM Beyer to enable the qualification of proliferating neuronal precursor cells[13]. All experimental procedures were conducted according to federal laws, and approved by the appropriate local authorities (LAGESO Berlin, Germany).

Experimental set-up.   The mice were randomly assigned to four different groups with a minimum of n = 5. After an adaption period, mice were placed into their assigned housing condition (Fig. 1A). The first group (IND) was housed in a simple standard cage (0.27 m × 0.15 m × 0.42 m) placed in the centre of a large enriched environment cage (0.74 m × 0.3 m × 0.74 m) and thus enabled to indirectly experience the stimulus-rich surrounding. The second group (DIR) was housed in the former mentioned enriched environment, enabled to directly experience and to physically interact with this stimulus-rich surrounding. IND and DIR were permanently confronted with each other and only separated by an acrylic Perspex wall and grids. The third group (ENR) was housed in an enriched environment cage (0.74m × 0.3m × 0.74m) similar to the one of the DIR group, but containing an uninhabited inner stand-ard cage. The fourth group (CTR) was housed in a standard cage (0.27 m × 0.15 m × 0.42 m) without any confrontation to environmental enrichment or any other mice and held under control conditions. Environmental enrichment was rearranged two to three times a week and consisted of a rearrangeable set of plastic tubes, cardboard tubes, grids, colourful cartons, varying shelters, and changing food and drinking places. All mice received food and water ad libitum and remained in a constant light/dark cycle of 12 hours. The standard cage housed 5 to 7 mice at the same time, while the ENR/DIR cage housed 5 to 10 mice at the same time. A total of 22 mice were used as CTR, four standard cages were used for this condition. A total of 23 mice were used as IND, four standard cages were used for this condition. A total of 22 mice were used as ENR, three ENR cages were used for this condition. A total of 29 mice were used as DIR, four DIR cages were used for this condition. A total of 26 transgenic GFP-nestin mice (CTR: N = 5, IND: N = 6, ENR: N = 5, DIR = 10) spent four weeks in the experiment and were used to analyse the proliferation of dividing precursor cells in the hippocampus. A total of 29 C57Bl/6 mice (CTR: N = 7, IND: N = 6, ENR: N = 7, DIR: N = 9) spent eight weeks in the experiment to assess the survival of newborn cells. A total of 41 C57Bl/6 mice were tested in the Morris water maze (CTR: N = 10, IND: N = 11, ENR: N = 10, DIR: N = 10) and visuo-spatial memory was assessed (Fig. 1B). The equipment of the room, experimentators and animal facility care personel remained stable over the whole experimental period.

BrdU-injection protocol.   To determine the proliferation and survival of newborn cells, mice were injected with 5-Bromo-2′-deoxyuridine (BrdU, Sigma) dissolved in 0.9% saline. BrdU is a thymidine analogon which incorporates into the DNA of dividing precursor cells and thus enables to assess prolifer-ating cells. The mice received three BrdU-injections (50mg/kg) intraperitoneally within twelve hours on day 28 of the experiment. The Nestin-GFP mice were transcardially perfused 24 hours after the injection in order to determine the proliferation rate of cells while the other mice were perfused four weeks after BrdU-injection to assess the survival of the newborn cells (Fig. 1B).

Histological tissue preparation.   All mice were deeply anaesthesized by an overdose of Ketamine and killed by transcardially perfusion with cold 0.1M phosphate-buffer saline (PBS, pH 7.4) followed by 4% paraformaldehyde. The mice were decapitated, the brains dissected, and stored for 24 hours in 4% paraformaldehyde for postfixation. After postfixation, the brains were dehydrated in 30% sucrose until they sunk to the bottom. Subsequently, the brains were frozen in liquid nitrogene and stored at −80°C till further processing. For histological analysis, the brains were cut into 40μm thick coronal sections using a cryostat (Leica DM 1850) and stored in cryprotectant at 4°C till staining.

Immunohistochemistry and analysis.   To quantify the number of newborn cells, one-in-a-6 series (240μm apart) of the sections were stained for BrdU-detection as described previously[12]. Sections were pretreated with 0.6% H_2O_2 for 30 minutes to block endogenous tissue peroxidase. After washing the free-floating sections in PBS, DNA was denatured with 2N HCL for 30 minutes at 37°C. The sections were then rinsed in borate buffer for 10 minutes followed by washing with PBS. To prevent unspecific antibody binding, sections were treated with PBS+ (0.1% TritonX-100, 3% donkey serum) for 30 min-utes before being incubated overnight with the primary antibody against BrdU (rat, Biozol) diluted 1:500 in PBS+. The primary antibody was washed out with PBS the next day. Subsequently, the sections were blocked again with PBS+ for 25 minutes followed by incubation with the biotinylated secondary anti-body (anti-rat, Dianova) diluted 1:250 in PBS+ for two hours at room temperature. After washing out the secondary antibody, avidin biotin peroxidase complex reagent (ABC Elite, Vector Laboratories) at a concentration of 9μl per 1ml PBS was applied for one hour and washed out. Diaminobenzidine (DAB, Sigma-Aldrich) was used as chromogene at the concentration of 0.025 mg/ml in destilled water and Tris-buffer with 0.01% H_2O_2 and 0.04% nickel chloride. After washing in PBS and destilled water, the free floating sections were mounted onto superfrost glass slides (Menzel), dehydrated in ascending con-centrations of ethanol, cleared in ProTaqs®Clear and coverslipped with ProTaqs®PARAmount. The same blinded researcher analysed DAB-stained sections for BrdU-positive cells throughout the rostrocaudal extent of the granule cell layer in both hippocampi except for the uppermost focal layer. The resulting number was multiplied by six to obtain an estimation of the total number of BrdU-positive cells in the dentate gyrus. Exemplary pictures of BrdU-positive cells were taken by differential interference contrast

(DIC)-microscopy (Olympus BX50). Unessential parts of the pictures were removed, but no further manipulation occurred.

Immunofluorescence staining and analysis. To determine the phenotype of the newborn cells, one-in-a-12 series (480µm apart) of the sections were double- or triple-labelled by the proliferating marker BrdU, the marker for mature neurons NeuN or marker for premature neurons Doublecortin, GFP for nestin-staining, and GFAP. After DNA denaturation, rinsing in borate buffer and blocking of unspecific antibody binding as described above, the sections were incubated overnight with the primary antibody diluted in PBS+ in the following concentrations: anti-BrdU 1:500 (rat, AbD Serotec), anti-NeuN 1:100 (mouse, Millipore), anti-GFP 1:250 (rabbit, Abcam), anti-Doublecortin 1:200 (goat, Santa-Cruz), anti-GFAP 1:200 (goat, Santa-Cruz). The next day, sections were rinsed followed by blocking with PBS+, and incubated with the secondary antibodies diluted in PBS+ at room temperature for four hours. The following secondary fluorochrome antibodies and concentrations were used: anti-rat Rhodamine X, 1:250 (Dianova), anti-mouse Alexa 488, 1:1000 (Invitrogen), anti-rabbit Alexa 488, 1:1000 (Invitrogen), anti-goat Alexa 647, 1:100 (Invitrogen). After incubation, sections were washed, mounted, dehydrated, cleared, and coverslipped. Immunofluorescence stained sections were analysed by taking confocal z-stacks scanned at 1µm intervals using a Leica TCS SP2. Fifty randomly selected BrdU-positive cells within the granule cell layer were investigated for co-expression of additional neuronal marker. The ratio of the neuronal phenotypes was multiplied by the total number of BrdU-positive cells and yielded an estimation of the absolute numbers of newborn neurons within the granule cell layer.

Behavioural testing and analysis. To assess spatial memory, a total of forty-one mice (CTR: N = 10, IND: N = 11, ENR: N = 10, DIR: N = 10) were tested in a modified reversal learning version of the Morris water maze as described previously[15]. For five consecutive days, mice were trained to navigate through opaque water to a hidden platform 1 cm below the surface of a circular tank (1.2m diameter). The temperature was kept constant at 19°C to 20°C. Every day consisted of six trials with a maximum duration of 120 seconds and an inter-trial interval time of 30 minutes. The starting position changed daily, but was kept constant during the day (Fig. 3D). The platform was relocated into the opposite quadrant on day four. In case a mouse failed to find the platform, it was guided to the platform and remained there for 15 seconds. Animals were tracked and recorded by Viewer[3] (Biobserve). The lengths of the swim paths to target and the number of crossings of the previous target zone were automatically analysed by Viewer[3]. To investigate qualitative properties of the learning in the Morris water maze, classification and analysis of search strategies were performed. Therefore, the recorded xy-coordinates were transferred into a Matlab-script (Mathworks, USA) and automatically analysed based on the algorithm elaborated previously[15]. Search strategies were classified as spatial or non-spatial strategies and chi-square-independence test was used to determine if groups performed more or less often spatial or non-spatial strategies as expected. Furthermore, the xy-coordinates were used to depict the spatial preference of the mice in heat maps of presence probability drafted automatically by the Matlab-script.

Statistical analysis and data presentation. Statistical analysis was performed in SPSS 21. The metric variables "number of cells" and "crossing of platform" were analysed with one-way ANOVA while the metric variable "length of swim path" was analysed using repeated measures ANOVA. For comparison between groups, post-hoc tests were used when main analysis revealed significance and Levene's test was performed to validate homogeneity of variances. Bonferroni-correction was chosen for post-hoc analysis in case of variance homogeneity and Tamhane's-T2 was selected in case of variance inhomogeneity. To determine an association between housing condition and the nominal variable hippocampal-dependent search strategy respectively hippocampal-independent search strategy the chi-square-independence test was applied. Therefore, the different search strategies were classified as hippocampal-dependent "spatial" strategies or as hippocampal-independent "non-spatial" strategies. According to the literature, the following strategies were defined as "spatial": "directed search", "focal search", "direct swimming" while the following strategies were defined as "non-spatial": "thigmotaxis", "random search", "scanning", "chaining"[15,27]. Likewise, chi-square-test was selected for assessment of "perseverance" and its association with housing conditions. For all applied statistical tests, the level of significance was set to the conventional level of 0.05. Absolute numbers of cells (Fig. 2B,C,E) and absolute numbers of platform crossings (Fig. 3A) are presented as boxplots with a center line as median, Tukey-style whiskers extend 1.5 times the interquartile range from 25th and 75th percentiles. The length of the swim path to reach the hidden platform is presented as mean+ s.e.m (Fig. 3B).

References

1. Kempermann, G., Kuhn, H. G. & Gage, F. H. More hippocampal neurons in adult mice living in an enriched environment. *Nature* **386,** 493–495 (1997).
2. Van Praag, H., Kempermann, G. & Gage, F. H. Running increases cell proliferation and neurogenesis in the adult mouse dentate gyrus. *Nature Neurosci* **2,** 266–270 (1999).
3. Fabel, K. *et al.* Additive effects of physical exercise and environmental enrichment on adult hippocampal neurogenesis in mice. *Front. Neurosci* **3,** doi: 10.3389/neuro.22.002.2009 (2009).
4. Kempermann, G., Kuhn, H. G. & Gage, F. H. Experience-induced neurogenesis in the senescent dentate gyrus. *J. Neuroscience* **18,** 3206–3212 (1998).

5. Van Praag, H., Christie, B. R., Seinowski, T. J. & Gage, F. H. Running enhances neurogenesis, learning, and long-term potentiation in mice. *Proc. Natl. Acad. Sci.* **96,** 13427–13431 (1999).
6. Nilsson, M., Perfilieva, E., Johansson, U., Orwar, O. & Eriksson, P. S. Enriched environment increases neurogenesis in the adult rat dentate gyrus and improves spatial memory. *J. Neurobiol* **39,** 569–578 (1999).
7. Laurin, D., Verreault, R., Lindsay, J., MacPherson, K. & Rockwood, K. Physical activity and risk of cognitive impairment and dementia in elderly persons. *Arch. Neurol* **58,** 498–504 (2001).
8. Radak, Z. *et al.* Exercise plays a preventive role against Alzheimer's disease. *J. Alzheimers Dis.* **20,** 777–783 (2010).
9. Freund, J. *et al.* Emergence of individuality in genetically identical mice. *Science* **340,** 756–759 (2013).
10. Rosenzweig, M. R., Bennett, E. L., Herbert, M. & Morimoto, H. Social grouping cannot account for cerebral effects of enriched environment. *Brain. Res.* **153,** 563–576 (1978).
11. Atienza, A. A. *et al.* Identifying sedentary subgroups: The NCI health information national trends survey. *Am. J. Prev. Med.* **31,** 383–390 (2006).
12. Lesemann, A. *et al.* MPTP-induced hippocampal effects on serotonin, dopamine, neurotrophins, adult neurogenesis and depression-like behavior are partially influenced by fluoxetine in adult mice. *Brain. Res.* **1457,** 51–69 (2012).
13. Yamaguchi, M., Saito, H., Suzuki, M. & Mori, K. Visualization of neurogenesis in the central nervous system using nestin promotor-GFP transgenic mice. *Neuroreport* **11,** 1991–1996 (2000).
14. Kempermann, G., Jessberger, S., Steiner, B. & Kronenberg, G. Milestones of neuronal development in the adult hippocampus. *Trends Neurosc.* **27,** 447–52 (2004).
15. Garthe, A., Behr, J. & Kempermann, G. Adult-generated hippocampal neurons allow the flexible use of spatially precise learning strategies. *PLoS One* **4,** e5464, doi: 10.137/journal.pone. 0005464 (2009).
16. Freund, J. *et al.* Association between exploratory activity and social individuality in genetically identical mice living in the same enriched environment. *Neuroscience.* doi:10.1016/j.neuroscience.2015.05.027 (2015).
17. Ferchim, P. A & Bennett, E. L. Direct contact with enriched environment is required to alter cerebral weights in rats. *J. Comp. Physiol. Psych.* **88,** 360–367 (1975).
18. Held, R. & Hein, A. Movement-produced stimulation in the development of visually guided behaviour. *J. Comp. Physiol. Psych.* **56,** 872–876 (1963).
19. Bednarczyk, M. R. *et al.* Distinct stages of adult hippocampal neurogenesis are regulated by running and the running environment. *Hippocampus* **21,** 1334–1347 (2011).
20. Kim, Y. *et al.* Association between various sedentary behaviours and all-cause, cardiovascular disease and cancer mortality: the Multiethnic Cohort Study. *Int. J. Epidemiol.* **42,** 1040–1056 (2013).
21. Wilmot, E. G. *et al.* Sedentary time in adults and the association with diabetes, cardiovascular disease and death: systematic review and meta-analysis. *Diabetologia* **55,** 2895–2905 (2012).
22. Sund, A. M., Larsson, B. & Wichstrøm, L. Role of physical and sedentary activities in the development of depressive symptoms in early adolescence. *Soc. Psychiatry. Psychiatr. Epidemiol.* **46,** 431–441 (2011).
23. Lindstrom, H. A. *et al.* The relationships between television viewing in midlife and the development of Alzheimer's disease in a case-control study. *Brain and Cognition* **58,** 157–165 (2005).
24. Bilimoria, P. M., Hensch, T. K. & Bavelier, D. A mouse model for too much TV? *Trends Cogn. Sci.* **16,** 529–531 (2012).
25. Cummins, R. A., Livesey, P. J. & Evans, J. G. A developmental theory of environmental enrichment. *Science* **197,** 692–694 (1977).
26. Christakis, D. A., Ramirez, J. S. B. & Ramirez, J. M. Overstimulation of newborn mice leads to behavioural differences and deficits in cognitive performance. *Sci. Rep.* **2,** 546, doi: 10.1038/srep00546 (2012).
27. Garthe, A., Huang, Z., Kaczmarek, L., Filipkowski, R. K. & Kempermann, G. Not all water mazes are created equal: cyclin D2 knockout mice with constitutively suppressed adult hippocampal neurogenesis do show specific spatial learning deficits. *Genes, Brain and Behavior* **13,** 357–364, doi: 10.1111/gbb.12130 (2014).

Acknowledgments

Author Contributions

D.I. performed the animal experiments and the data-analysis and wrote the manuscript, C.K. conducted the behavioral testing, A.G. provided the analytical tools for the behavioral testing, Y.W. supported behavioral testing and manuscript revision, G.K. initiated the study, provided the equipment for the experiment and wrote the manuscript, B.S. conceived and designed the study and wrote the manuscript.

Additional Information

Curriculum vitae

Mein Lebenslauf wird aus datenschutzrechtlichen Gründen in der elektronischen Version meiner Arbeit nicht veröffentlicht.

List of Publications

Research Articles	**Hain EG, Klein C, Braun J, Riek K, Müller S, Sack I, Steiner B.** Dopaminergic neurodegeneration in the mouse is associated with decrease of viscoelasticity of substantia nigra tissue. PLoS One 11:e0161179.
	Klein C, Rasińska J, Empl L, Sparenberg M, Poshtiban A, Hain EG, Iggena D, Rivalan M, Winter Y, Steiner B. 2016. Physical exercise counteracts MPTP-induced changes in neural precursor cell proliferation in the hippocampus and restores spatial learning but not memory performance in the water maze. Behav Brain Res 307:227-238.
	Klein C, Jonas W, Iggena D, Empl L, Rivalan M, Wiedmer P, Spranger J, Hellweg R, Winter Y, Steiner B. 2016. Exercise prevents high-fat diet-induced impairment of flexible memory expression in the water maze and modulates adult hippocampal neurogenesis in mice. Neurobiol Learn Mem 131:26-35.
	Iggena D, Klein C, Garthe A, Winter Y, Kempermann G, Steiner B. 2015. Only watching others making their experiences is insufficient to enhance adult neurogenesis and water maze performance in mice. Sci Rep 5:14141.
	Klein C, Hain EG, Braun J, Riek K, Müller S, Steiner B, Sack I. 2014. Enhanced adult neurogenesis increases brain stiffness: in vivo magnetic resonance elastography in a mouse model of dopamine depletion. PLoS One 9:e92582
	Klein C, Karanges E, Wong A, Spiro A, Spencer J, Huynh T, Gunasekaran N, Karl T, Long LE, Xuang X-F, Liu K, Arnold JC, McGregor IS. 2011. Cannabidiol potentiates Δ9-Tetrahydrocannabinol (THC) behavioural effects and alters THC pharmacokinetics during acute and chronic treatment in adolescent rats. Psychopharmacology (Berlin) 218:443-57.
	Brosda J, Hayn L, Klein C, Koch M, Meyer C, Schallhorn R, Wegener N. 2011. Pharmacological and parametrical investigation of prepulse inhibition of startle and prepulse elicited reactions in rats. Pharmacol Biochem Behav 99:22-8.
Conference Contributions **(Poster Presentation)**	**Klein C, Rasińska J, Empl L, Sparenberg M, Poshtiban A, Iggena D, Winter Y, Rivalan M, Flöel A, Steiner B.** Physical activity increases adult hippocampal neurogenesis and spatial

learning in a mouse model of Parkinson's disease. 12th International Conference on AD/PD, Nice, March 2015.

Hain EG, Sparenberg M, Klein C, Steiner B. Modulating effects of indomethacin on neurogenesis in the 1-methyl-4-phenyl-1,2,3,6-tetrahydropyridine mouse model. 9th FENS Forum of Neuroscience, Milan, July 2014.

Klein C, Empl L, Iggena D, Winter Y, Rivalan M, Flöel A, Steiner B. Effects of physical activity on adult hippocampal neurogenesis and cognitive flexibility in a mouse model of Parkinson's disease. 11th International Conference on AD/PD, Florence, March 2013.

Klein C, Jonas W, Wiedmer P, Huehnchen P, Maurer L, Spranger J, Steiner B. Diet- and exercise-modulated alterations of neurogenesis in mouse hypothalamus and hippocampus. 8th FENS Forum of Neuroscience, Barcelona, July 2012.

Klein C, Huehnchen P, Maurer L, Spranger J, Steiner B. Effects of physical activity and nutrition on neural plasticity and neurogenesis in the healthy brain and in a mouse model of Parkinson's disease. SfN Annual Meeting, Washington D.C., November 2011.

Klein C, Karanges E, Huyhn T, Spencer J, Gunasekaran N, Arnold JC, Long LE, Karl T, McGregor IS. Pretreatment with cannabidiol enhances Δ^9-THC behavioural effects and blood levels in adolescent rats. 20th Annual Symposium on the Cannabinoids, Lund, July 2010.

Wong A, Gunasekaran N, Klein C, Radford J, McGregor IS, Arnold JC. Delta-9-tetrahydrocannabinol but not olanzapine induces adipocyte hypertrophy and macrophage infiltration. Attenuating actions of co-administered cannabindiol. 11th Australasian Schizophrenia Conference, Sydney, September 2010.

Conference Contributions **(Oral Presentation)**	**Klein C, Jonas W, Wiedmer P, Huehnchen P, Maurer L, Spranger J, Steiner B.** Ernährungs- und Körperaktivitäts-assoziierte Veränderungen der Neurogenese im Hypothalamus und Hippocampus der Maus. 85th Congress of the German Society of Neurology, Hamburg, September 2012.